



HAL
open science

The nature of the Moho beneath fast-spreading centers: Evidence from the Pacific plate and Oman ophiolite

Yoshihiko Tamura, Mathieu Rospabé, Gou Fujie, Akane Ohira, Kentaro Kaneda, Alexander Nichols, Georges Ceuleneer, Tomoki Sato, Shuichi Kodaira, Seiichi Miura, et al.

► To cite this version:

Yoshihiko Tamura, Mathieu Rospabé, Gou Fujie, Akane Ohira, Kentaro Kaneda, et al.. The nature of the Moho beneath fast-spreading centers: Evidence from the Pacific plate and Oman ophiolite. *Island Arc*, 2022, 31 (1), 10.1111/iar.12460 . hal-03807990

HAL Id: hal-03807990

<https://hal.science/hal-03807990>

Submitted on 13 Oct 2022












HAL is a multi-disciplinary open access archive for the deposit and dissemination of scientific research documents, whether they are published or not. The documents may come from teaching and research institutions in France or abroad, or from public or private research centers.

L'archive ouverte pluridisciplinaire **HAL**, est destinée au dépôt et à la diffusion de documents scientifiques de niveau recherche, publiés ou non, émanant des établissements d'enseignement et de recherche français ou étrangers, des laboratoires publics ou privés.



Distributed under a Creative Commons Attribution - NonCommercial - NoDerivatives 4.0 International License

The nature of the Moho beneath fast-spreading centers: Evidence from the Pacific plate and Oman ophiolite

Yoshihiko Tamura¹  | Mathieu Rospabé¹  | Gou Fujie¹  | Akane Ohira¹  |
 Kentaro Kaneda²  | Alexander R. L. Nichols³  | Georges Ceuleneer⁴  |
 Tomoki Sato¹  | Shuichi Kodaira¹  | Seiichi Miura¹  | Eiichi Takazawa^{1,5} 

¹IMG, JAMSTEC, Yokosuka, Japan

²Japan Coast Guard, Tokyo, Japan

³School of Earth and Environment, University of Canterbury, Christchurch, New Zealand

⁴CNRS-UMR5563-Toulouse University, Toulouse, France

⁵Niigata University, Niigata, Japan

Correspondence

Yoshihiko Tamura, IMG, JAMSTEC, Yokosuka 237-0061, Japan.

Email: tamura@jamstec.go.jp

Present address

Mathieu Rospabé, Geo-Ocean, Univ Brest, CNRS, Ifremer, UMR6538, Plouzané, France.

Akane Ohira, INPEX, Tokyo, Japan.

Funding information

Japan Society for the Promotion of Science, Grant/Award Numbers: JP16H02742, JP16H06347, JP17H02987, JP21H01195

Abstract

It is common knowledge that the Moho is the boundary between the crust and the Earth's mantle. Here we show along several seismic profiles through the Pacific Plate that a correlation exists between the strength of Moho reflections, crustal thickness, and water depth. Where the Moho can be detected clearly, the overlying oceanic crust is systematically thicker and the water depths are shallower. We suggest that two end-members of oceanic crust exist in fast spreading environments: one thick, underlain by a clear Moho; the other thinner, without a Moho; with all intermediate situations. In the Oman ophiolite, the best-preserved on-land analogue of fossil oceanic lithosphere created by fast-spreading, the boundary between the mantle peridotites and the lower crustal gabbros mainly consists of a dunitic transition zone (DTZ) ranging from a few meters to a few hundred meters in thickness. A sudden influx of seawater down to the base of the crust at the mid-ocean ridge (MOR) results in the hydrous (re-)melting of mantle peridotites, producing a dunitic residue at the crust–mantle boundary that represents the most reflective Moho. At the same time, the hydrous melting, in addition to the normal decompression melting, beneath the MOR, increases the thickness of the oceanic crust by enhancing magma production. In the absence of hydrous melting, the DTZ is thin or absent at the crust–mantle boundary, and instead the uppermost mantle harzburgite is intruded by gabbros, and/or the overlying crustal gabbro is intruded by numerous wehrlite bodies, which will be seismically gradational.

KEYWORDS

boninite, crust–mantle boundary, dunite, hydrous melting, Moho, Oman ophiolite, Pacific Plate, Penrose model, seismic profile, seismic reflections

1 | INTRODUCTION

Participants of an international Penrose Field Conference on ophiolites in September 1972 produced a consensus statement that defined

an ophiolite from bottom to top to be: (1) ultramafic rocks of the upper mantle, consisting of variable proportions of harzburgite, lherzolite and dunite; (2) layered and isotropic gabbros; (3) a sheeted dike complex (diabase); and (4) basaltic lavas, commonly pillowed

This is an open access article under the terms of the [Creative Commons Attribution-NonCommercial-NoDerivs](https://creativecommons.org/licenses/by-nc-nd/4.0/) License, which permits use and distribution in any medium, provided the original work is properly cited, the use is non-commercial and no modifications or adaptations are made.

© 2022 The Authors. Island Arc published by John Wiley & Sons Australia, Ltd.

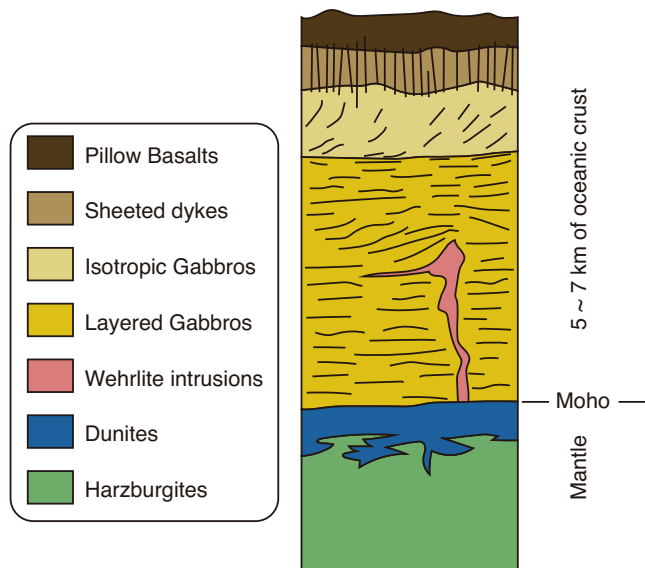


FIGURE 1 The “Penrose-type” ophiolite showing a layer-cake pseudo-stratigraphy represented by the Samail ophiolite, Sultanate of Oman (e.g., Boudier & Nicolas, 1985; Dick et al., 2006). The Moho is defined as a boundary between dunites and the gabbros

(Conference participants, 1972). The Oman ophiolite (Samail ophiolite, Sultanate of Oman) fits this layer-cake “Penrose-type” ophiolite pseudo-stratigraphy (e.g., Boudier & Nicolas, 1985; Dick et al., 2006; Dilek & Furnes, 2011), shown in Figure 1. Christensen and Smewing (1981) recognized that the thickness and seismic properties of the igneous oceanic crust and upper mantle in the Samail ophiolite were similar to those of Pacific crust and upper mantle formed at intermediate- to fast-spreading ridges.

Kempner and Gettrust (1982) suggested that synthetic seismograms for the Samail ophiolite velocity-depth functions and observations from the ROSE refraction data from the East Pacific Rise have striking similarities, and that ophiolites represent good analogues of the oceanic lithosphere. If this is the case, the petrologic features that are responsible for oceanic crustal and upper mantle seismic structures can be observed directly in ophiolites (Christensen & Smewing, 1981). The assumption has developed that the Penrose-type ophiolites are ancient and largely intact sections of oceanic crust and upper mantle created at fast spreading mid-ocean ridges (MORs) preserved on land (e.g., Dick et al., 2006; Dilek, 2003; Michibayashi et al., 2019): this is called the Penrose model, which is now a widely accepted paradigm.

Our target in this paper is to verify that the Penrose model faithfully represents the petrology of the Oman ophiolite and accurately models fast-spreading MORs. The Moho is defined as a boundary between the lower crust (layered gabbros) and the uppermost mantle (dunites). Crustal accretion processes at MORs differ from fast-through slow- to ultraslow-spreading ridges. While the Penrose model is widely accepted for the Pacific crust created at fast-spreading ridges (Dick et al., 2006), Cannat (1996) and Cannat et al. (1997)

proposed that the lower crust generated at slow-spreading ridges consists of serpentinized peridotite variably intruded by gabbroic bodies and overlain by a thin veneer of pillow basalt with a poorly developed or absent sheeted dike complex.

A major limitation in determining the nature and origin of the Moho in the present-day oceanic lithosphere is the scarcity of rock samples from the crust–mantle transition or boundary to compare with the geophysical survey data. The petrology of the oceanic crust–mantle interface has been mostly established in specific geotectonic contexts where the lower crust, crust–mantle transition and even the uppermost mantle outcrop on the seafloor, are exhumed along detachment faults of oceanic core complexes at slow to ultra-slow spreading centers (e.g., Dick et al., 2003; Sauter et al., 2013) or are exhumed along transform faults at spreading centers with various accretion rates (e.g., Bonatti et al., 2003; Bonatti & Honnorez, 1976; Cannat et al., 1990; Cipriani et al., 2009; Maia et al., 2016; Mével et al., 1991). In these cases, samples are frequently overprinted by deformation, as well as fluid-rock and/or melt-rock interactions potentially related to the exhumation itself. The accretion of a heterogeneous igneous oceanic lithosphere potentially shows the characteristics of slow-spreading ridges (e.g. Cannat, 1996; Ildefonse et al., 2007), and on-land versions of such incomplete oceanic crust may be exemplified by the Alpine ophiolites (Dilek & Furnes, 2011; Ishiwatari, 1985a, 1985b, and references therein), which did not necessarily form at fast-spreading ridges. Hard-rock deep drillings in the oceanic crust had been designed to test the Penrose model. However, only four holes in the entire international ocean drilling program have penetrated the oceanic crust beyond 1 km, but no further than 2 km (Dick et al., 2006; Michibayashi et al., 2019). A more ambitious project (“MoHole”), whose aim is to reach the Moho beneath 5–6 km of crust, was proposed more than 60 years ago and has still not been achieved. In this context, the comparison of geophysical survey data with petrological and geochemical features (together with field and structural observations) characterizing ophiolites that accreted in various contexts and were created at spreading centers spreading at a variety of rates, especially fast spreading rates, is essential for petrologists and geophysicists to reach an accord on the nature of the Moho.

Combined studies of the seismic structure of the Pacific Plate and the petrology of the Oman ophiolite are the best approach to advance our knowledge of MORs and to test the Penrose model. Based on this, there is still much that is a matter for debate. We present here new seismic studies of Moho reflections in the Pacific Plate and show that the Moho reflections are not ubiquitous features. Then, we interpret the results in the light of recent petrological, geochemical and structural observations in the Oman ophiolite.

2 | OVERVIEW OF THE MOHO IN PRESENT-DAY OCEANS

“The origin of the Moho has been debated since its discovery, and the debate is still ongoing” (Prodehl et al., 2013). The Moho is a major

global seismic discontinuity between Earth's crust and upper mantle, discovered by and named after the Croatian seismologist Andrija Mohorovičić (1910). An enthusiasm and genuine curiosity were stimulated regarding the nature of the materials on either side of the discontinuity since its discovery (Jarchow & Thompson, 1989). The continental Moho is beyond the scope of this paper. The nature of the crust–mantle boundary in cratonic regions remain enigmatic, due to a lack of key xenoliths or exposed sections, and the Moho does not necessarily coincide with the base of the continental crust (O'Reilly & Griffin, 2013). We focus on the oceanic Moho produced at fast-spreading MORs.

Hess (1962) proposed that the oceanic Moho is a boundary between fresh and serpentinized peridotite, which makes the seismic Moho deeper than the crust–mantle boundary. Coleman (1971) rejected Hess' model based on the heat flow recorded along the axis of oceanic ridges (Lee & Uyeda, 1965) combined with the evidence that the amount of water in the mantle is exceedingly low. O'Reilly et al. (1996) suggested that the shallow mantle below the Rockall Trough of the northeastern Atlantic Ocean developed a zone of partially serpentinized upper mantle peridotites not above, but beneath, the Moho. The Moho was not displaced by the zone of serpentinization, which has a velocity of 7.5–7.8 km/s and higher V_p/V_s and became shallower toward the edges of the trough. More recently, the fact that the Moho is a boundary between serpentinized and fresh peridotites has been shown partly to be valid at slow spreading rates but that the water was coming from hydrothermal fluids (Cannat, 1993).

Since 1980, the position of the Moho in the oceanic lithosphere has been determined almost exclusively by seismic refraction measurements (Oliver, 1982), although Stoffa et al. (1980) used reflections in multi-channel seismic data that are continuous beneath the axial zone of the active East Pacific Rise near 9° N to suggest that the Moho forms nearly contemporaneously with the oceanic crust. Collins et al. (1986) investigated the origin and characteristics of oceanic Moho reflections by computing two-dimensional synthetic seismogram profiles of the inferred fossil oceanic crust/mantle transition observed in the Bay of Islands ophiolite, western Newfoundland. The synthetic multiphase Moho reflection events are laterally discontinuous on a scale similar to that observed in the western North Atlantic, suggesting that the structures observed in the inferred fossil crust/mantle transition of the ophiolite are characteristic of oceanic lithosphere (Collins et al., 1986). Brocher et al. (1985) calculated synthetic seismograms that model vertical-incidence seismic reflections in the oceanic Moho from detailed laterally varying velocity–depth models of two ophiolite complexes, the Bay of Islands ophiolite, in Newfoundland, and the Rustaq massif in the Samail ophiolite. Their principal result was that the observed lateral variability of seismic reflections from the oceanic Moho can be explained primarily by lateral variations in the geology at the Moho (Brocher et al., 1985). The nature of Moho reflections of the Pacific Plate, produced at fast spreading centers, could thus reflect the nature and variation of the materials that should be juxtaposed across the Moho in the Oman ophiolite.

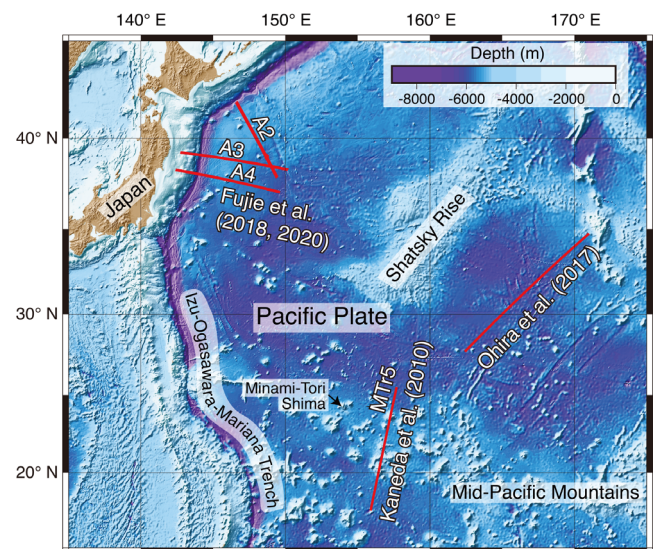


FIGURE 2 Solid red lines show seismic reflection and refraction profiles conducted by JAMSTEC and Japan coast guard in the northwestern Pacific Ocean, which have been examined in this study. The seismic reflection and refraction survey line by Ohira et al. (2017) was approximately 1130 km long, which is one of the longest single seismic profiles in the northwestern Pacific, and it spans old Pacific plate ranging from 148 Ma, at the southwestern end, to 128 Ma at the northeastern end. Strong and continuous Moho reflections were only observed at the southwestern end of the profile (for about 50 km), whereas Moho reflections were diffuse, weak, or absent along the rest of the profile (about 1080 km). The survey line (MTr5) by Kaneda et al. (2010) crossed two large seamounts, Batiza and Tayama guyots in the Marcus-wake seamount chain, and also includes Jurassic oceanic seafloor in the northern basin (about 159 Ma), at the northern end, and in the southern basin (about 167 Ma), at the southern end. These two basins have significantly different Moho reflections and crustal thickness. A2, A3, and A4 are seismic survey lines studied by Fujie et al. (2018, 2020). This part of the Pacific plate was formed at 130–140 Ma at a fast-spreading ridge. The appearance of the Moho reflections and crustal thickness are variable in the region 200–400 km along the profile

3 | MATERIALS AND QUESTIONS

Seismic waves reflect at a boundary between two distinct layers with contrasting acoustic impedances, which have been induced by large differences in densities and seismic velocities. The lower oceanic crust, essentially gabbroic, and the shallow mantle below it, which is deemed to be composed of spinel peridotite, have acoustic impedances of about 22 and 28 MPa s m⁻¹, respectively (e.g., Yamane et al., 2012). Thus, the boundary or transition between the gabbro and peridotite is supposed to be reflective enough to represent the Moho. However, seismic profiles generally show that Moho reflections are not universal, and many places in the world appear to lack a Moho in reflection data. Is this an imaging problem or is the Moho actually missing?

We have reviewed and examined several seismic survey profiles in the Pacific Plate, which have been conducted by JAMSTEC and the Japan Coast Guard (Figure 2). To avoid or reduce the imaging

problems, which may result from different sea and/or weather conditions and by using different methods or specifications, reflection and refraction images are compared within individual survey lines. Notably, the same seismic survey lines can show both strong and weak reflections. We suggest that if the Moho is missing this is not an imaging problem, instead different types of crust–mantle boundary actually exist: some are reflective and many others are not. We have also discovered a relationship between the dynamics of Moho reflectivity, the overlying crustal thickness, and the water depth. The oceanic crust is thicker and the water depth is shallower where the Moho has a strong reflectivity.

As the Oman ophiolite and the Pacific Plate both formed at fast-spreading centers, the clear relationship between the strong seismic reflections at the Moho and the thicker overlying crust in the Pacific Plate can be explored using the Oman ophiolite dunitic transition zone (DTZ) as an exposed analogue in which hypotheses and models of formation can be more easily tested. Starting with the hypothesis that fluid-melt-rock reactions generate a thicker DTZ (rather than simply melt-rock reaction), which is the main petrological process discussed here for the origin of the crust–mantle dunitites, we will now discuss how such processes may be responsible for strong Moho reflections on one hand, and weak or no Moho reflections on the other hand.

We present a new hypothesis for how the crust–mantle boundary forms at fast spreading MORs, which explains why below thick oceanic crust there are strong Moho reflections, and, conversely, below thin oceanic crust there are weak or no Moho reflections.

4 | ANALYTICAL METHODS USED: EXPERIMENTS AND DATA PROCESSING

The seafloor topography (water depth) was derived from the multi-narrow beam bathymetric data obtained during the individual survey cruises.

4.1 | The profile of Ohira et al. (2017)

In 2014, JAMSTEC carried out a multichannel seismic reflection (MCS) survey using R/V *Kairei* along a 1130 km-long survey line on the northwestern part of the Pacific Plate southeast of the Shatsky Rise. The survey vessel fired a tuned air-gun array with a total volume of 130 L at a spacing of 200 m. The seismic signals were recorded by a 5.5 km-long, 444-channel hydrophone streamer cable (hydrophone spacing was 12.5 m) towed by the vessel and five ocean bottom seismometers (OBSs) equipped with a three-component geophone and a hydrophone sparsely deployed along the profile. The depths of the air-gun array and streamer cable were 10 and 12 m, respectively.

4.2 | MTr5 of Kaneda et al. (2010)

The MCS survey and wide-angle seismic reflection and refraction survey using OBSs were individually conducted by the Hydrographic and

Oceanographic Department, Japan Coast Guard (JCG) in 2006. A tuned air-gun array with a total volume of 132 L was used as a controlled seismic source for both of MCS and OBS surveys. During the MCS survey, R/V *Tairikudana* fired the air-gun array at every 50 m and towed a 6-km-long streamer cable with 480 channels (receiver interval 12.5 m) at a depth of 12 m. One hundred eighty OBSs equipped with a three-component geophone and a hydrophone were deployed at 5 km intervals. The shooting interval for the OBSs was 200 m and the depth of the air-gun array was 10 m.

4.3 | A2, A3, and A4 of Fujie et al. (2018, 2020)

Since 2009, JAMSTEC has conducted several MCS and OBS surveys at the outer rise of the Japan and Kuril Trenches on the oceanic Pacific Plate along lines up to as several hundred kilometers long (Fujie et al., 2013, 2018; Kodaira et al., 2014). MCS data were collected using the same system as Ohira et al. (2017), but the shooting interval was 50 m. To collect the wide-angle seismic reflection and refraction data, OBSs were deployed at 6 km interval along lines A2, A3, and A4; the total numbers of OBSs were 80, 86, and 80, respectively. The air-gun depth for OBS data was 12 m and shot interval was 200 m.

4.4 | Data processing

The MCS data were processed following conventional procedures including datum correction, band-pass filtering, predictive deconvolution (JAMSTEC data) or signature deconvolution (JCG data), amplitude recovery, common midpoint sorting, velocity analysis, parabolic Radon demultiple, normal moveout correction, stacking, and post-stack time migration.

First internal clocks of each OBS were calibrated by using GPS time recorded just before release and after retrieval. Then positions of the OBSs on the seafloor were determined by an inverse calculation using arrival times of direct water waves and seafloor topography. For travel-time picking, band-pass filter and predictive deconvolution were applied. Seismic velocity models were derived by forward modeling (Ohira et al., 2017), by travel-time inversion using first arrivals and Moho reflections (Fujie et al., 2013, 2018, 2020), or by a combination of travel-time inversion and forward modeling (Kaneda et al., 2010). See the relevant references for more details.

5 | MOHO REFLECTIONS, CRUSTAL THICKNESSES, AND WATER DEPTHS IN THE PACIFIC OCEAN

The relationships between Moho reflections, crustal thickness, and water depth have been investigated in studies from three different areas of the northwestern Pacific Ocean (Ohira et al., 2017; Kaneda et al., 2010; Fujie et al., 2018, 2020). Additionally, a summary of the Moho reflections beneath the East Pacific Rise (EPR) is provided in Section 5.4.

5.1 | Southeast of the Shatsky rise

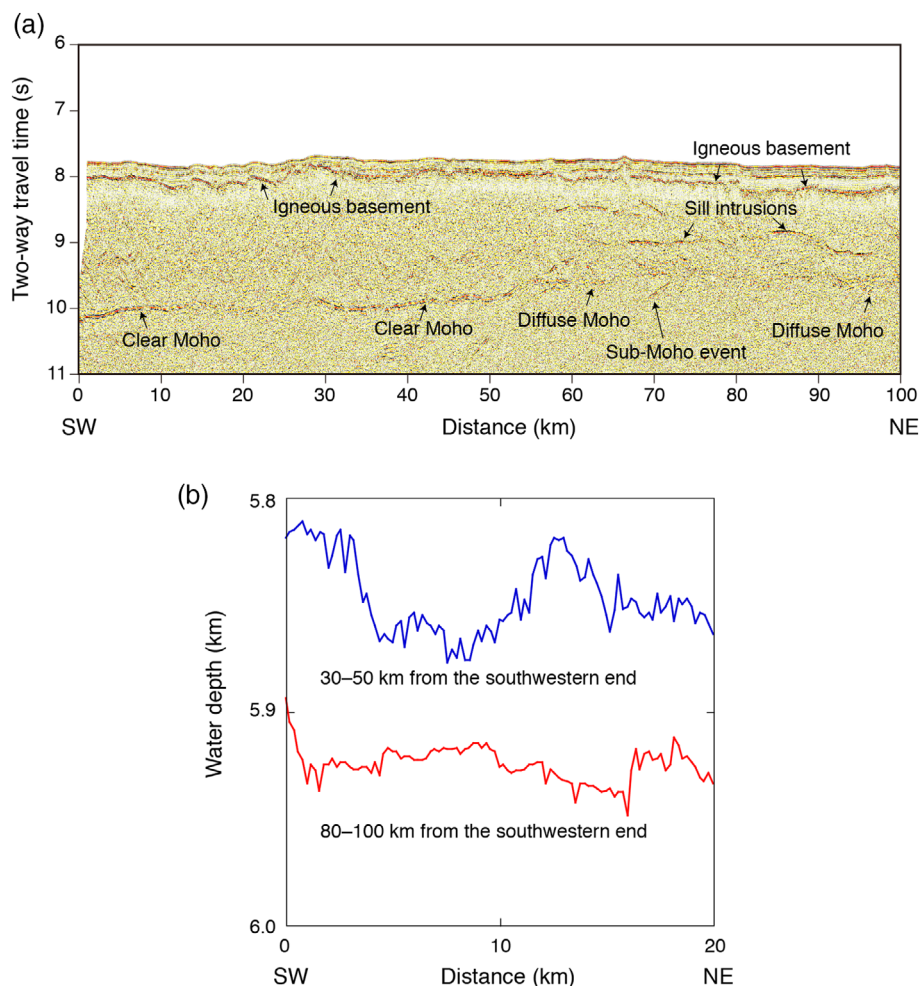
Ohira et al. (2017) studied Moho reflections in a typical ocean basin produced at a MOR, which is located about 600 km southeast of the Shatsky Rise (Figure 2) and perpendicular to the Hawaiian magnetic anomalies. Their seismic reflection survey line was approximately 1130 km long, which is one of the longest single seismic profiles in the northwestern Pacific. It spans old Pacific Plate ranging from 148 Ma to 128 Ma, from the southwestern to the northeastern end, respectively. The oceanic crust was formed at the Pacific-Farallon spreading ridge, with a half spreading rate estimated to be fast to intermediate, and constant at about 40 mm year^{-1} (Nakanishi et al., 1992). Strong and continuous Moho reflections are observed only at the southwestern end of the profile (about 50 km in length), whereas Moho reflections are diffuse, weak, or absent along the rest and most of the profile (about 1080 km). Figure 3 shows the MCS image of the first 100 km of the profile after Ohira et al. (2017), including the first 50 km where the Moho reflections are sharp, single, flat, and continuous, and of large amplitude. At 60 km along the profile, the Moho reflections change from clear to diffuse northeastwards. A sub-Moho event, which could be gabbroic intrusions, or more generally mafic intrusions, in the uppermost mantle, and sills

within the crust are observed from 60 to 100 km along the profile. Crust is thick in the section from 0 to 50 km, but is thin in the section from 60 to 100 km along the profile. Ohira et al. (2017) showed that “At 55 km distance, clear Moho reflections become 250 ms TWTT (two-way travel time) shallower within a horizontal range of a few kilometers, although the seafloor topography is smooth and the igneous basement has little roughness.” Along the profile from the southwestern end, the seafloor becomes younger from M20 (146 Ma) to M19 (145 Ma) and the average water depth increases from $5847 \pm 18 (1\sigma) \text{ m}$ (30–50 km from the southwestern end) to $5925 \pm 7 (1\sigma) \text{ m}$ (80–100 km from the southwestern end) (Figure 3b), which coincides with the decrease in crustal thickness. Thus, where the Moho reflections change from strong/clear to weak/diffused, crustal thickness changes from thick to thin, and water depths also become deeper.

5.2 | Across the Marcus-Wake seamount chain

Kaneda et al. (2010) conducted seismic surveys across the Marcus-Wake seamount chain in the northwestern Pacific Ocean. The survey line (MTR5) crossed the centers of two large seamounts, Batiza and

FIGURE 3 Multi-channel seismic reflection (MCS) image of the southwestern-most 100 km of the profile from Ohira et al. (2017). (a) The clear Moho reflections from 0 to 50 km along the profile are characteristically sharp, single, flat, and continuous, and of large amplitude. At 60 km the Moho reflections become diffuse (Ohira et al., 2017). The sub-Moho event, which could be gabbroic intrusions into the uppermost mantle and sills in the crust, are observed from 60 to 100 km. Crustal thickness decreases from 0–50 km to 60–100 km. (b) Water depth (km) versus distance from the southwestern end of the seismic line by Ohira et al. (2017). The region 30–50 km along the profile, where the Moho reflections are clear, has an average depth of $5847 \pm 18 (1\sigma) \text{ m}$, and the region 80–100 km, where the Moho reflections are weak or absent $5925 \pm 7 (1\sigma) \text{ m}$. thus, the areas with strong Moho reflections have shallower water depths than those where the Moho reflections are weak or absent, suggesting that the depth of water is related to crustal thickness via isostasy



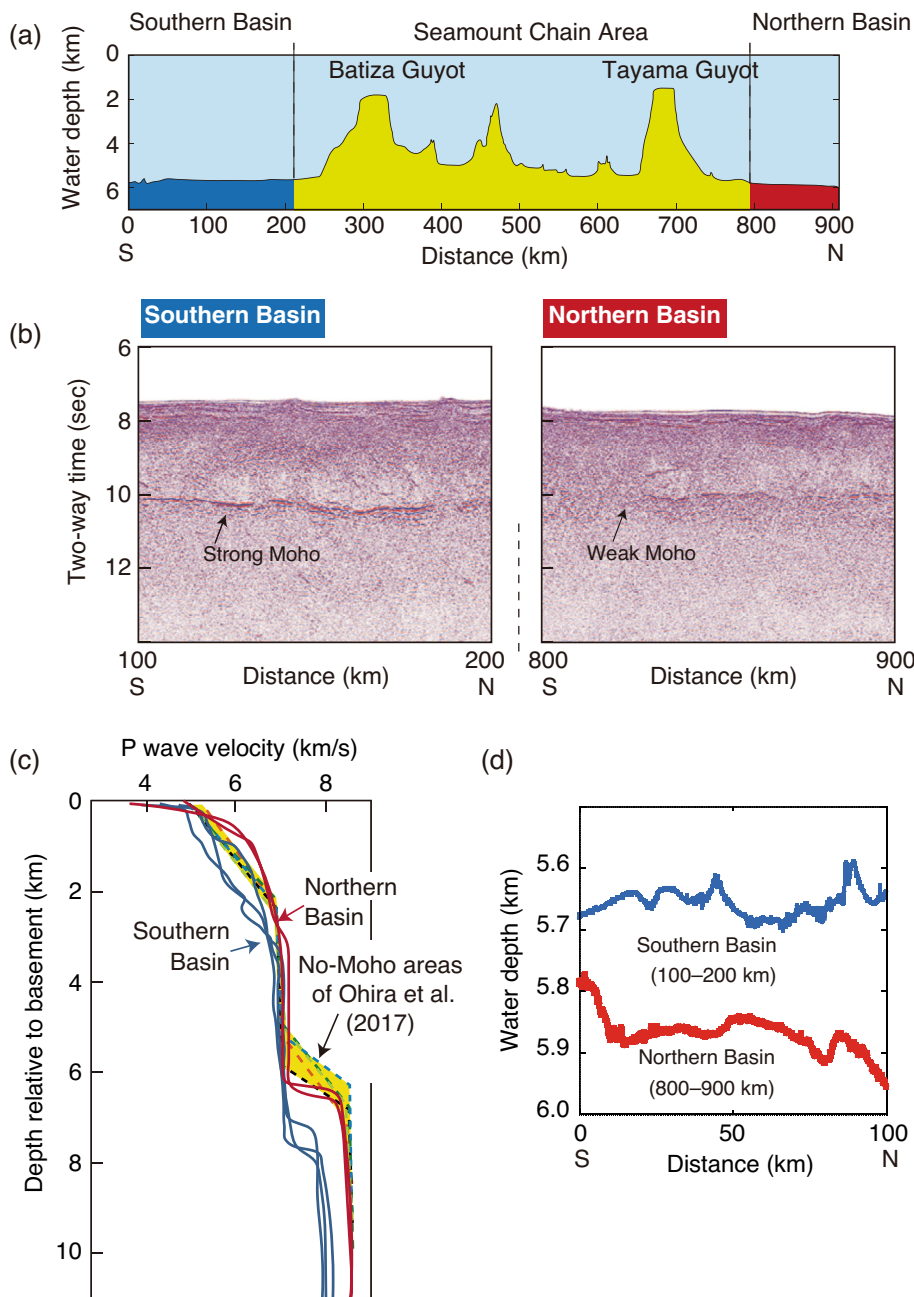


FIGURE 4 Seismic surveys across the Marcus-wake seamount chain in the northwestern Pacific Ocean.

(a) Bathymetry along line MTr5. Kaneda et al. (2010) referred to the line segments 0–210 km, 210–790 km, and 790–910 km as the southern basin, seamount chain, and northern basin, respectively. (b) The southern and northern basins have contrasting multi-channel seismic reflection (MCS) profiles. The southern basin from 100–200 km shows strong and continuous Moho reflections, but the Moho is weak below the northern basin from 800–900 km. (c) P-wave velocity profiles of the southern and northern basins from MTr5 from Kaneda et al. (2010) and where the Moho is absent in the profile of Ohira et al. (2017). Crust of the southern basin is 7.5–8 km thick, which is 1.5–2 km thicker than that of the northern basin. The crust where the Moho is absent in the profile of Ohira et al. (2017) is also much thinner than that in the southern basin. Moreover, the changes of P-wave velocity from lower crust to upper mantle are not sharp, but have a gentle slope where Moho reflections are not observed (Ohira et al., 2017). (d) Water depth versus distance in the southern and northern basins. Average water depth in the southern basin is 5657 ± 21 (1σ) m and 5870 ± 30 (1σ) m in the northern basins, respectively. The southern basin has a reflective Moho, thick oceanic crust and shallow water. The northern basin is the opposite

Tayama guyots, in the vicinity of Minami-Tori Shima, which is the easternmost Japanese island and the only one on the Pacific Plate (Figure 2). This seismic line includes Jurassic oceanic seafloor at both its northern and southern ends (framing the seamount chain area), which were referred to as the northern and southern basins (Figure 4a). Magnetic anomalies suggest Jurassic ages of M32 (159 Ma) and M42 (167 Ma) for the northern and southern basins, respectively. These two basins have significantly different Moho reflections, crustal thicknesses, and water depths (Figure 4b–d). The southern basin has clear Moho reflections, which are characteristically sharp, single, flat, and continuous, and of large amplitude. In the northern basin Moho reflections are extremely weak or even absent (Figure 4b). Interestingly, the crust of the southern basin has a

constant thickness of about 7.5–8.0 km, whereas the crust of the northern basin has a constant thickness of 6 km, 1.5–2 km thinner than that of the southern basin (Figure 4c). Figure 4c compares the P-wave velocity profiles in the southern and northern basins from MTr5 from Kaneda et al. (2010) with the areas where the Moho is absent in the profile from Ohira et al. (2017). The areas where the Moho is absent in the Ohira et al. (2017) profile have a much thinner crust compared to the southern basin. Moreover, the changes in the P-wave velocities from the lower crust to the upper mantle are not sharp, but have a gentle slope where Moho reflections are not observed (Ohira et al., 2017). Figure 4d shows the depth of water according to the distance along the profile. Average water depths in the southern and northern basins are 5657 ± 21 (1σ) m and 5870

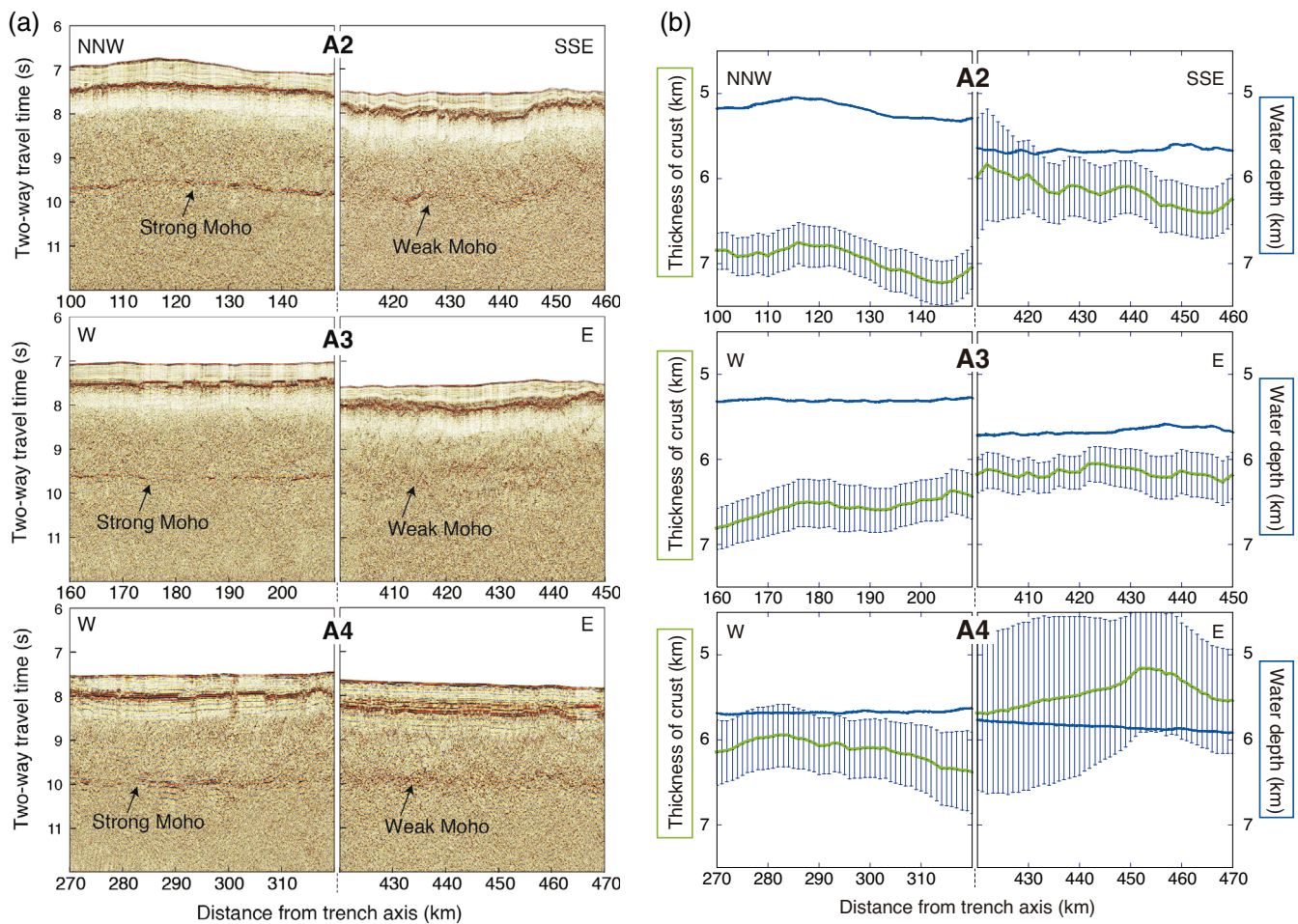


FIGURE 5 (a) Representative 50-km segments of the time-migrated multi-channel seismic reflection (MCS) profiles from seismic survey lines A2, A3, and A4 of Fujie et al. (2018, 2020), showing strong Moho reflections (left) and weak Moho reflections (right) of the Pacific Ocean floor off East Japan. The vertical axis shows two-way travel time (seconds), the horizontal axis is the distance from the trench axis (km). (b) Crustal thickness (km) (green line) and water depth (km) (blue line) for the same representative 50-km segments as shown in (a). Crustal thickness estimated from seismic refraction studies, error bars show one standard deviation. To avoid or reduce the imaging problems, reflection and refraction images have been compared within individual survey lines. In each seismic survey line, the crust is thicker by a few hundred meters to a kilometer and water depths are shallower where Moho reflections are strong. The 100–150 km segment of A2 has the strongest Moho reflections, the thickest crust (about 7 km), and the shallowest water depth

± 30 (1σ) m, respectively. The southern basin has a reflective Moho, thick oceanic crust and shallow water depths. The northern basin is the opposite. The differences between the northern and southern basins are similar to those observed by Ohira et al. (2017) in their seismic profile, with strong Moho reflections coinciding with thicker oceanic crust and shallower water depths than that with weak Moho reflections.

5.3 | East of Japan

The area of the Pacific Plate that was surveyed by Fujie et al. (2018, 2020) was formed between 130 and 140 Ma at a fast spreading ridge (Nakanishi, 2017). Figure 5a shows representative time-migrated MCS reflection profiles from seismic survey lines A2, A3, and A4 of the Fujie et al. (2018, 2020) studies. Moho reflections and crustal thickness are variable at 200–400 km along the lines. Sections from each profile displaying strong (left) and weak (right) Moho reflections have been

extracted. The two-way travel times of the top of the seafloor also suggest that the seafloor is shallower where the Moho reflections are strong. The diagrams in Figure 5b show the thickness of the overlying crust and the depth of water for the sections of the profiles shown in Figure 5a. The 100–150 km section of A2 has the strongest Moho reflections, the thickest crust (about 7 km) and the shallowest water depths. Oceanic crust ranges from about 5 to 7 km in thickness (Figure 5b), but in each seismic survey line, the crust is systematically thicker, by about a few hundred meters to one kilometer, and water depths systematically shallower, where Moho reflections are stronger compared to the areas where the Moho reflections are weak or absent.

5.4 | East Pacific rise (EPR)

Dunn et al. (2000) showed the three-dimensional seismic structure and physical properties of the crust and shallow mantle beneath

the EPR at 9°30' N and estimated the thermal structure and melt distribution beneath the spreading center. They suggested a substantial increase in width of the high-temperature and melt-containing regions from the lower crust to the mantle, indicating that the focused ascent of magma had a strong local influence on the accretion of oceanic crust.

Using three-dimensional seismic reflection images, Singh et al. (2006) reported the presence of Moho reflections beneath a crustal magma chamber at the 9°03' N overlapping with the spreading center of the EPR. The presence of the Moho very close to or even exactly beneath the ridge crest implies that it was formed at essentially zero age (Mutter & Carton, 2013).

A recent 3D seismic reflection study at the EPR, between 9°42' N and 9°57' N and extending ~12 km away from the ridge axis shows that the character of the Moho reflections vary from impulsive to shingled to diffuse, even in this newly formed crust where spreading rate is constant and far from any plume activity (Aghaei et al., 2014). This variation is interpreted by these authors to reflect variations in accretion processes, for example, efficient mantle melt extraction to the crust forms the impulsive Moho character, while crustal accretion models from multiple magma bodies can explain the diffused Moho character (Aghaei et al., 2014). In their figure 12, Aghaei et al. (2014) showed that in the southern area between 9°42' N and 9°48' N the crust is ~5550 m thick, which is 100–200 m thicker than it is in the northern area between 9°52' and 9°56'. The Moho reflections are also stronger and shingled in the southern area compared to the northern area.

5.5 | Systematic relationships between Moho reflections, crustal thickness, and water depths

Figure 6 shows a schematic diagram to summarize the relationship between Moho reflections, oceanic crustal thicknesses and water depths deduced from the seismic profiles described above. Moho reflections return from the boundaries between the lowermost crust and uppermost mantle. A thick oceanic crust overlays strong Moho reflections, and weak or no Moho reflections are observed at the base of a thin oceanic crust. Moreover, seafloor tends to be shallower where the crust is thicker even though the formation ages of thick and thin crust are similar, suggesting that the water depth is related to crustal thickness via isostasy.

Acoustic impedance is a product of density multiplied by P-wave velocity. The strong Moho reflections could result from a large and sudden change in the acoustic impedance at the boundaries as shown on the left of Figure 6. Where Moho reflections are weak or absent there could be a gradual change in the acoustic impedance at the boundaries as shown on the right of Figure 6. Can these different acoustic impedances at the crust–mantle boundaries be related to variations in geochemistry and petrology? How are the crustal thicknesses related to the acoustic impedance at the boundaries?

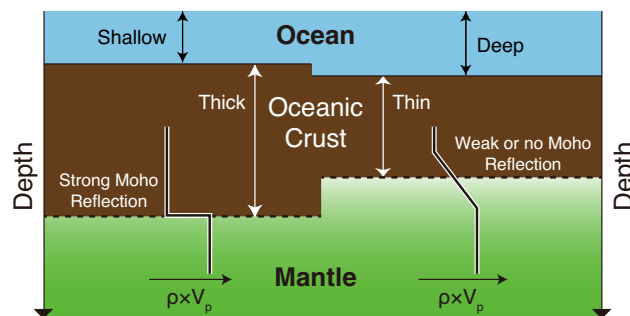


FIGURE 6 A schematic diagram to summarize the relationship between Moho reflections, crustal thickness and water depth in seismic profiles. Thick oceanic crust has strong Moho reflections at its base; thin oceanic crust weak or no Moho reflections at its base. Water depths tend to be shallower when the crust of the same age is thicker. Moho reflections are sent back from the boundaries between the lowermost crust and uppermost mantle. Strong Moho reflections could result from a large and sudden change in the acoustic impedance (density multiplied by P wave velocity, $\rho \times V_p$) at the crust–mantle boundary as shown on the left of the diagram. Where the Moho reflections are weak or absent, the change in the acoustic impedance across the boundary is more gradual as shown on the right of the diagram.

6 | THE BOUNDARY BETWEEN THE OCEANIC CRUST AND THE MANTLE IN THE OMAN OPHIOLITE

6.1 | Oman ophiolite

The Oman ophiolite is the largest and best-preserved ophiolite worldwide (Figure 7). It is a remnant of the Tethys oceanic crust that accreted c. 95 Ma (e.g., Rioux et al., 2012, 2013, 2016; Tippet et al., 1981). Among other petrological and structural evidence, the thickness of the crust (about 5 km thick on average)—especially its continuous layered gabbro section (3.6 km thick on average; Nicolas et al., 1996)—has been used as a strong argument for the crust to have originated at a fast spreading center (Boudier et al., 1997; Ceuleneer, 1986; Ceuleneer et al., 1988; MacLeod & Rothery, 1992; Nicolas et al., 1988; Pallister & Hopson, 1981; Smewing, 1981; Tilton et al., 1981). As a result, the Oman ophiolite has regularly been compared to the East Pacific Rise (e.g., Boudier et al., 1997; Pallister & Hopson, 1981). The petrology and geochemistry of the crust–mantle transition above a fossil mantle diapir that fed the main mid-ocean ridge basalt (MORB) segment of the Oman ophiolite has been widely studied, especially recently (e.g., Rospabé et al., 2017, 2018; Rospabé, Benoit, et al., 2019; Rospabé, Ceuleneer, et al., 2019), which makes this part of the ophiolite a particularly good candidate to understand the processes operating at the Moho beneath highly productive spreading centers that are likely to be fast spreading.

6.2 | Dunitic transition zone (DTZ)

In the Oman ophiolite, the boundary between mantle peridotites and layered gabbros from the lower oceanic crust is not sharp, but mainly

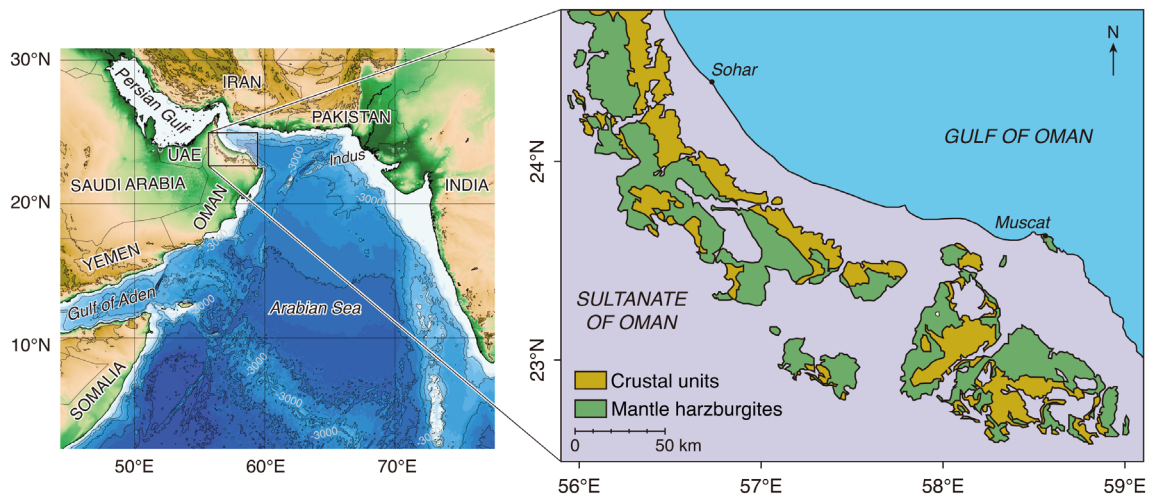


FIGURE 7 The Oman ophiolite along the northern coast of the Sultanate of Oman is the largest and best sub-aerial exposure of oceanic crust and upper mantle in the world. Crustal units consist of pillow basalts, sheeted dikes, and gabbroic plutonic rocks. Mantle harzburgites represent residual upper mantle peridotites that underwent partial melting to form the magmas that comprise the overlying igneous oceanic crust. The boundary between mantle harzburgites and layered gabbros from the lower oceanic crust (the Moho boundary) is not sharp, but mainly consists of a dunitic transition zone (DTZ) as shown in Figure 1. The right diagram is modified from Nicolas et al. (2009). The left locality map is by courtesy of Natsue Abe

consists of a DTZ. Dunite is a rock dominated by olivine with a few percent of scattered chromite and variable amounts of interstitial plagioclase and clinopyroxene, which may locally occur in high enough abundances for the rock to be classified as troctolite or wehrlite. In this context, dunite at the mantle–crust transition has been mainly interpreted to be a mantle-derived rock (e.g., Abily & Ceuleneer, 2013; Boudier & Nicolas, 1995; Godard et al., 2000; Koga et al., 2001; Rabinowicz et al., 1987; Rospabé et al., 2017, 2018; Rospabé, Benoit, et al., 2019), i.e. formerly a residual harzburgite that has been depleted in orthopyroxene due to reaction with a percolating melt and/or fluid (e.g. Dick, 1977; Kelemen, 1990). This reaction can be described as the transformation of an orthopyroxene crystal into solid olivine + liquid silica. In reality, the reaction is more complex due to the relatively high content of minor elements in orthopyroxene, mostly Al and Cr, that will distribute into newly formed chromite crystals and the silica-rich melt. This reaction is accompanied by a significant increase in permeability as olivine is more easily “wetted” by an interstitial melt than orthopyroxene leading to a higher permeability of dunite compared to harzburgite and lherzolite. Dunite is thus an efficient media for the extraction of melts from the mantle to the oceanic crust, while cooling may lead to the crystallization of interstitial minerals, such as plagioclase and clinopyroxene (e.g., Ceuleneer et al., 1996; Kelemen et al., 1995).

6.3 | Thick DTZ

The thickness of the DTZ in Oman ranges from a few meters to a few hundred meters (Boudier & Nicolas, 1995; Rabinowicz et al., 1987). Along the ophiolite, there are several areas where the foliations and lineations of the mantle peridotite have been imprinted during

asthenospheric flow; they are perpendicular to the paleo-Moho and have been interpreted to be paleo-mantle diapirs (Ceuleneer et al., 1988). The thickness of the DTZ appears to be higher above the diapirs and to decrease away from these structures (Ceuleneer, 1991). In off-axis positions above the thinnest crust–mantle transitions, more numerous wehrlite bodies originating from the DTZ and intruding into the overlying crustal gabbroic cumulates have been observed and interpreted as extracted materials related to the compaction of the dunitic mush (e.g., Benn et al., 1988; Joussetin & Nicolas, 2000; Juteau et al., 1988). A synoptic survey across the crustal section and DTZ has shown that the thinnest crust (actually the thinnest gabbro units, assuming that extrusive basalts and the sheeted dike complex have a constant thickness) is underlain by the thickest DTZ, particularly in the southeastern massifs of the ophiolite (Nicolas et al., 1996), but it is not always easy to define precisely the upper limits of the DTZ because of the plagioclase impregnations and greater concentration of gabbro sills and intrusions in the upper part of the DTZ. Thus, a thick DTZ does not always correspond to a thick “purely” dunitic layer.

6.4 | Hydrous mantle melting

A particularly thick DTZ (>300 m) has developed above the Maqсад mantle diapir in the Sumail massif, southeast of the Oman ophiolite (Ceuleneer & Nicolas, 1985; Rabinowicz et al., 1987). The Maqсад diapir is located at the center of a former ridge segment that was 80 km long and, at a maximum, 30 km wide. This segment was fed with melt that has a clear MORB affinity (Benoit et al., 1996; Ceuleneer et al., 1996; Python et al., 2008; Python & Ceuleneer, 2003). In addition to the interstitial plagioclase and clinopyroxene between olivine

grains in the DTZ dunites (Abily & Ceuleneer, 2013; Boudier & Nicolas, 1995; Koga et al., 2001), consistent with a MORB igneous environment, orthopyroxene and amphibole are believed to have crystallized from the interstitial melt (Rospabé et al., 2017). This suggests crystallization under hydrous conditions, which is unexpected as the troctolitic and gabbroic cumulates cropping out deeper in the mantle section in this area are believed to have crystallized from a dry MORB derived from partial melting of the Maqсад diapir (Benoit et al., 1996; Ceuleneer et al., 1996). A possible explanation to account for the phases derived from water- and silica-rich parent melts, restricted to the crust–mantle transition, is the mixing between MORB and more silicic hydrous melts produced by the re-melting of the partially serpentinized shallowest mantle (Amri et al., 1996; Benoit et al., 1999). The higher abundance up-section along the DTZ of mineral phases that are exotic in a MORB environment is consistent with the water being seawater in origin, and connected to hydrothermal systems (Rospabé et al., 2017). When the mantle melts under hydrous conditions the liquidus field of forsterite expands relative to that of enstatite and incongruent melting of enstatite is triggered, producing high amounts of dunites and andesitic and even more silica-rich melts, the latter now crystallized as tonalite-trondhjemites pods and dikes.

The similar nature of the silicate minerals (mostly amphibole, orthopyroxene and mica) included within newly formed chromite supports the involvement of a hydrated and silica-rich component (Borisova et al., 2012; Rospabé et al., 2017, 2020; Rospabé, Ceuleneer, et al., 2019; Yao et al., 2020). Old chromite grains in some ophiolites are diamond-bearing and were produced at depths greater than 400 km, and the mineral inclusions in such chromites may have more complex histories (e.g., Arai, 2010; Arai, 2013; Lian & Yang, 2019; Miura et al., 2012; Robinson et al., 2004; Yamamoto et al., 2009; Yang et al., 2007). These are not relevant to this study, and we focus on newly formed chromite grains that crystallized in the uppermost mantle beneath MORs.

The hydrated component within chromite may be involved at an early stage, as the dunite and chromite forms at the expense of harzburgite, probably enhancing the (fluid-) melt–rock reaction, and is likely to be responsible for the petrological and geochemical diversity within the DTZ (Rospabé et al., 2017, 2018). Moreover, the vertical evolution of the petrology and geochemistry in the Maqсад DTZ strongly correlates with the presence of fault zones, highlighting that the DTZ dunites (and chromites) formed by the interaction between three main processes: (1) magmatism; (2) high temperature hydrothermal activity; and (3) faulting. This process of faulting, active over a wide range of temperatures from magmatic to very low-grade metamorphic conditions (e.g., Abily et al., 2011; Zihlmann et al., 2018), makes the hybridization of hydrothermal-derived fluids and mantle-derived silicate melts possible (Rospabé, Benoit, et al., 2019; Rospabé, Ceuleneer, et al., 2019). Hybridization may thus contribute to the formation of a thicker DTZ beneath oceanic spreading centers.

In the early work on the Oman ophiolite, the thicker DTZ was interpreted to be solely the result of more melt being delivered to the spreading center by the partially melted mantle diapir. Primarily, thin oceanic crust results from low degrees of partial melting of the

mantle, and thick oceanic crust from high degrees of partial melting. In the Maqсад area, however, while there is evidence of intense magmatic activity related to the paleo-diapir and the thick DTZ (i.e. numerous mafic dikes and/or melt percolation features), there is also more abundant evidence for hydrated magmatism (producing orthopyroxene, amphibole, chromites) at the top of the diapir (contrasting with the troctolitic cumulates that crystallized from a MORB parent melt deeper in the mantle; Benoit et al., 1996; Clénet et al., 2010; Rospabé et al., 2017). Potential explanations are that: (1) a more developed mantle diapir better reheats the base of the cold lithosphere, previously partially hydrothermally altered during alternating magmatic and tectonic-hydrothermal cycles, and thus better “recycles” or re-involves the fluid fractions with the newly produced silicate melts; (2) an along-axis migration of the upwelling mantle materials; or (3) a combination of both, during spatially and temporally varying magmatic activity along the spreading center. In consequence and according to field, structural and petrological/geochemical observations in the Oman ophiolite, a thick DTZ apparently resulted from an abundant supply of both MORB and hydrothermal fluids. Thus the thickness of the DTZ beneath oceanic ridges might be correlated to the thickness of the overlying crust.

7 | REVIEW OF HYDROUS PARTIAL MELTING IN A MOR SETTING

There is evidence of interactions between seawater, or seawater-derived fluids, and the oceanic crust in present-day MOR settings, triggering the hydrous partial melting of the already (partially or completely) crystallized surrounding rocks (Benoit et al., 1999; Nonnotte et al., 2005). At shallow levels, the introduction of seawater is mainly responsible for the pervasive alteration of the MORB and the underlying sheeted dike complex (SDC) (e.g., Alt et al., 1986). The felsic intrusions (i.e., plagiogranites) at the transition between the SDC and the gabbros, and within the upper gabbroic sequence, are attributed to the anatexis of the altered, hydrated mafic rocks by a new magma pulse following an amagmatic, tectono-hydrothermal cycle (e.g., France et al., 2009, 2013; Koepke et al., 2007; Wanless et al., 2010; Zhang et al., 2017).

Deeper in the oceanic crust orthopyroxene and amphibole crystals have been observed locally along olivine, plagioclase and clinopyroxene grain boundaries in layered gabbros (Koepke et al., 2005). At high temperatures (near 1000°C), this is explained by the water-rich fluids propagating along grain boundaries and triggering hydrous, incongruent partial melting of the primary minerals (Koepke et al., 2005, 2014). This reaction is indeed accompanied by the crystallization of both orthopyroxene and amphibole from the newly formed water- and silica-rich melt fraction. Experimental work confirms the plagiogranitic nature of the melt associated with such fluid-melt-rock reactions (Wolff et al., 2013). Interestingly, the presence of discrete amphibole and orthopyroxene crystals in present-day oceanic gabbros has been observed in crust created at MORs with different spreading rates; from slow spreading ridges, such as the Mid-Atlantic Ridge or

the Southwest Indian Ridge, to the faster spreading East Pacific Rise (Koepke et al., 2005).

It has been proposed that such seawater-derived fluids, triggering the hydrous partial melting of surrounding rocks, can reach the uppermost mantle in MOR settings. First observed in the MORB part of the Oman ophiolite (Benoit et al., 1999), similar gabbro cumulates have been identified along the Mid-Atlantic Ridge as the crystallization product from an andesitic melt produced by hydrous melting of the shallow mantle (Nonnotte et al., 2005). Their Nd isotopic compositions are consistent with the parent melt originating from a depleted N-MORB mantle source, while their Sr isotopes reflect seawater being introduced throughout the magmatic evolution of the system during partial melting and fractional crystallization.

To summarize, the hydrous partial melting of mafic and/or ultramafic rocks beneath MORs occurs along what can be called a “metamorphic interface” between the downgoing hydrothermal front and MORB uprising from partial melting of the deeper mantle (i.e., on-axis melt lens in the case of the SDC-gabbro transition, e.g., Koepke et al., 2009).

8 | ROCK TYPES AND MOHO REFLECTIONS

8.1 | Dunite

A “pure dunite,” mainly made of olivine and a few percent of chromite, and thus devoid of melt migration features (e.g., plagioclase, clinopyroxene), would have a density similar to mantle peridotites, and slightly higher than, and thus with a greater contrast to the density of crustal gabbros. In this way, a thick dunite would produce strong and sharp Moho reflections.

If there is: (1) a well-developed mantle diapir; and (2) stronger involvement of the hydrated component in the fluid-melt-rock reaction leading to the mantle harzburgite dunitization (Rospabé et al., 2017), more magma will be produced, which will result in thicker overlying crust and a thicker dunite.

8.2 | Troctolite in DTZ and wehrlite in gabbro

Where the DTZ includes melt migration features, interstitial minerals (e.g., plagioclase, clinopyroxene, orthopyroxene, amphibole) between olivine grains (e.g., Abily & Ceuleneer, 2013; Boudier & Nicolas, 1995; Koga et al., 2001; Rospabé et al., 2017), such as in the Maqсад area, troctolite and/or wehrlite modal compositions are reached, which do not have such a strong contrast to crustal gabbros. The Maqсад DTZ consists of lower “pure dunites” and upper “impregnated dunites” (Rospabé, 2018; Rospabé, Benoit, et al., 2019). The density of a strongly impregnated dunite will be intermediate between peridotites and crustal gabbros, resulting in a gradual decrease in density across the DTZ from the mantle to the crust, producing diffuse Moho reflections.

The thickness of the impregnated DTZ could decrease due to the compaction of the mush in off-axis areas (Benn et al., 1988; Joussetin & Nicolas, 2000; Juteau et al., 1988). This compaction process expels the interstitial material that will crystallize in the crust as wehrlite intrusions upsection, sometimes causing the base of the crust to become a hybrid between the partially crystallized gabbro and the wehrlite (e.g., Juteau et al., 1988).

8.3 | Serpentinized peridotite

A thicker DTZ has the potential (i.e., the high abundance of olivine) to allow a thicker serpentine-rich layer to develop as the result of the circulation of significant amounts of low-temperature seawater and subsequent serpentinization. This will have a big impact on the seismic data (e.g., Minshull et al., 1998). The recent drilling of the Oman ophiolite during the Oman Drilling Project (Kelemen et al., 2020), recovered altered and extensively serpentinized dunite from the mantle-derived DTZ. This has a higher permeability than the serpentinized harzburgites from the mantle section (Katayama et al., 2020). The difference is significant enough that it would be detected using seismic instruments in present-day oceanic lithosphere as shown by O'Reilly et al. (1996), but to date such high permeabilities have not been measured in the oceanic mantle. In the model, we propose here for fast-spreading ridges, the role of hydrothermal fluids is important but as we invoke processes that take place at very high temperature, above the stability of serpentine, serpentinization is not expected to play a major role compared to dunitization.

9 | NEW HYPOTHESIS FOR THE MOHO FORMATION

We present a new three-stage hypothesis to explain the formation of the Moho beneath fast-spreading centers. (1) An accidental and sudden influx of hydrothermal water to the crust–mantle boundary triggered by faulting results in the hydrous re-melting of depleted mantle peridotite and, possibly, previously crystallized and altered gabbroic rocks. (2) The formation of dunite at the crust–mantle boundary is related to the destabilization of orthopyroxene induced by the hydrous re-melting of depleted upper mantle peridotite, which is dramatically enhanced by the addition of water in the system, and the reaction between the mantle peridotite and migrating MORB under-saturated in pyroxene at low pressure. The development of this thick dunite layer, analogous to those observed in ophiolites, may represent the clearest and most reflective Moho. (3) The addition of melts (and eventually cumulates) produced by hydrous melting of shallowest mantle, the efficient extraction of melts from the mantle to the oceanic crust through permeable dunites, and the development of deep crustal mafic/ultramafic cumulates increases the thickness of the oceanic crust. In addition, the formation of a DTZ could be enhanced at the top of mantle diapirs, resulting in a thicker DTZ. Consequently, dunites and a reflective Moho correlate with thicker crust.

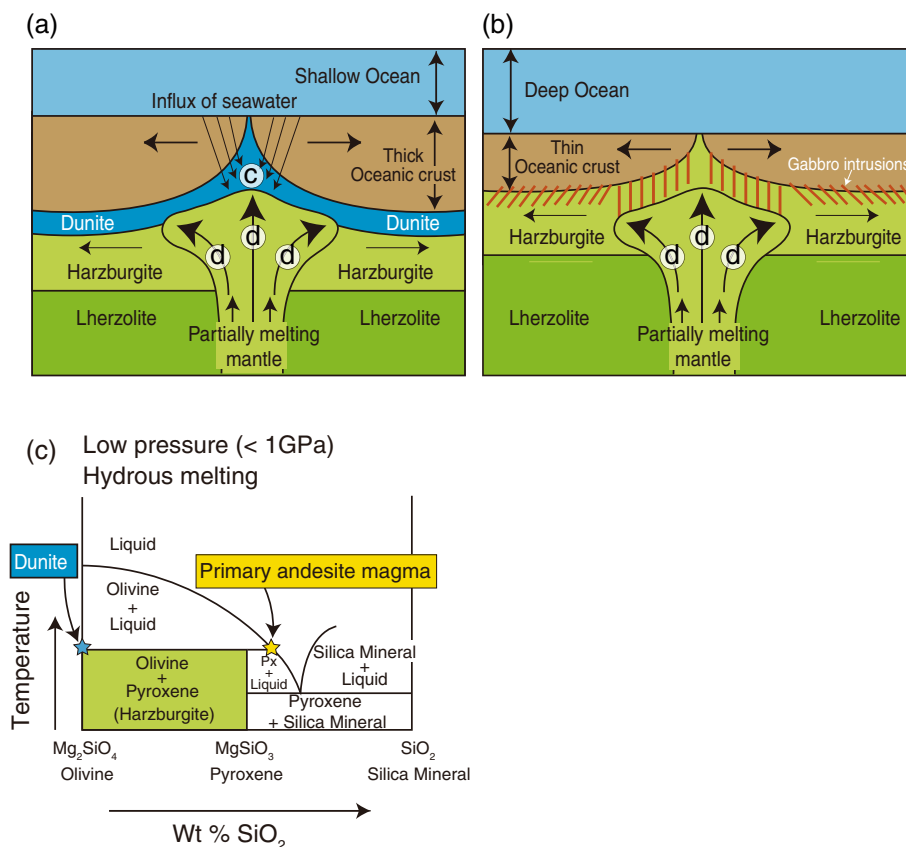


FIGURE 8 Schematic diagrams explaining the relationship between crustal thickness and the crust–mantle boundary. These diagrams provide the basis for a revised 3D Penrose model. The crust–mantle boundary in the Oman ophiolite ranges from (a) thick dunite layers to (b) many mafic/ultramafic intrusions within mantle harzburgite and the lower crust. The thick dunite layers will give strong Moho reflections, resulting in a clear Moho, but many mafic/ultramafic intrusions will cause a gradual change in the acoustic impedance, resulting in weak or no Moho reflections. The water depths tend to be shallower when the crust is thicker probably due to isostatic response. (a) A model to produce thick crust and thick dunite layers. © indicates hydrous melting, @ decompression melting. Decompression melting of the upwelling mantle (@) is the major process that produces MORB magmas and oceanic crust. In addition to this process, seawater could infiltrate into the shallowest mantle through normal faults at the MOR. Incorporation of water into the mantle will lower the solidus and could trigger mantle melting (©), which otherwise cannot occur, to produce primary andesite magmas (see (c)). (b) A model to produce thin crust and gabbroic intrusions at the crust–mantle boundary. Decompression melting of upwelling mantle (@) is the major process. Red bars show a swarm of gabbroic intrusions within the uppermost mantle harzburgite, which grade to crustal cumulates. Thus, the boundary between the lower crust and upper mantle is seismically gradational. A swarm of wehrlite intrusions within the lower crustal gabbro could also make the seismically gradational boundary. (c) at low pressure and under hydrous conditions, the liquidus field of olivine expands relative to that of enstatite, with the result that enstatite melts incongruently to produce primary andesite magma and dunite

Figure 8 shows schematic diagrams that explain the relationship between crustal thicknesses and the nature of the crust–mantle boundaries. These diagrams provide the basis for a revised 3D Penrose model. The crust–mantle boundaries in the Oman ophiolite range from two endmember configurations: (1) a thick (a few hundred meters) dunite layer with rare gabbroic sills; and (2) a swarm of gabbroic sills or more generally mafic intrusions within mantle harzburgite grading to crustal cumulates (cf. Akizawa et al., 2016; Rabinowicz & Ceuleneer, 2005). The former will cause strong Moho reflections, while the latter will induce gradual changes in the acoustic impedance, which finally result in weak or no Moho reflections. The influx of seawater at MORs (Figure 8a) can thus produce the thick crust and thick dunite layers at the same time.

Decompression melting of upwelling mantle, shown as @ in Figure 8a,b, is the major process that results in the genesis of MORB magmas and in the formation of oceanic crust. In addition to this process, the infiltration of seawater into the shallowest mantle could be enhanced by normal faults that are a common feature at MORs (Figure 8a). The incorporation of water into the mantle rocks lowers their solidus, making melting of the peridotite and primitive cumulates, which are quite refractory and cannot usually melt in dry conditions, possible. Hydrous melting of harzburgites produces magmas with the composition of a depleted, high-Mg andesite or boninites (Figure 8c).

Boninites are found in many ophiolites, the on-land remnants of the oceanic lithosphere (Ishiwatari, 2010). This should have led scientists to investigate whether it is possible that boninite magmas can

erupt in a MOR setting. Initially ophiolite complexes were thought to have been created at MORs (e.g., Dewey & Bird, 1971). However, the presence of boninites pointed scientists in a different direction. Miyashiro (1973) proposed that the Troodos ophiolitic complex formed in an island arc. This was based on the presence of tholeiitic and calc-alkalic series rocks in the Troodos ophiolite, as found in volcanic arc lavas, whereas mid-ocean ridge lavas all belong to the tholeiitic series. Pearce and Robinson (2010) summarized the debate about the origins of the Troodos ophiolite complex. They concluded that the Troodos ophiolite is comprised of magmas from the boninitic and tholeiitic series, not tholeiitic and calc-alkalic series as advocated by Miyashiro (1973), and that the Troodos ophiolite formed in a subduction initiation or slab edge setting rather than an island arc setting.

Boninites have not been found at MORs, or in crust generated at MORs. We think the reason for this is the andesitic melts, which are the outgrowth of dunites (Figure 8c), mix with much more dominant basaltic melts extracted from the deeper parts of the melting column. However, Benoit et al. (1999) shows that there are some rocks, including cumulates, at MORs that appear to be the residuum of melts that contain more silica and are much more depleted in incompatible elements than MORB. We believe that these observations indirectly suggest that boninites are produced beneath MORs and thus the presence of boninites in the Troodos ophiolitic complex does not rule out formation in a MOR setting and the idea that ophiolites can form in MOR settings should rise from the dead.

In contrast, normal decompression melting results in thin crust and mafic, mostly gabbroic intrusions at the crust–mantle boundary (Figure 8b). In dry conditions, a melt resulting from 15% to 20% of partial melting of a peridotite and multiply saturated with olivine, spinel and both ortho- and clinopyroxene in the pressure range of 2.5–1.0 GPa has the composition of an olivine tholeiite. With increasing pressure, the partial melt will become more Mg-rich and silica-poor (e.g., Presnall et al., 1979; Stolper, 1980). MORBs are complex mixtures of melt fractions whose compositions evolve continuously in the melting column during the decompression melting process. This is due to the combined effect of: (1) the evolution of the multiple saturation points toward compositions richer in silica with decreasing pressure; and (2) the progressive depletion of the source as partial melting progresses (e.g., Grove et al., 1992). Although the andesitic melts, which are the outgrowth of dunites (Figure 8c), would be mixed with much more dominant basaltic melts extracted from the deeper parts of the melting column (Figure 8a), there must be systematic and significant differences between crustal materials where the Moho is present and where it is absent.

Tamura et al. (2016, 2019) suggests that shallow melting of hydrous mantle and primary andesite magma generation could be responsible for continental crust formation in subduction zones. Such mantle melting results in residual dunites and plays a role in producing reflective boundaries in the oceanic crust (Figure 8a). Although the mechanism for hydrating the mantle is quite different, the recipe for mantle melting (Figure 8c) to form the continental crust and the oceanic Moho is similar.

10 | CONCLUSIONS

Based on new seismic studies, we show that Moho reflections are rare, not ubiquitous, features in the Pacific Plate. Below thick oceanic crust the Moho reflections are strong, whereas below thin oceanic crust they are weak or absent. These results are interpreted in the light of recent petrological, geochemical and structural observations in the Oman ophiolite. The crust–mantle boundaries in the Oman ophiolite range between two endmember configurations: (1) a thick dunite layer with rare gabbroic sills; and (2) a swarm of gabbroic sills, or more generally mafic intrusions, within mantle harzburgite grading into crustal cumulates. The former will cause strong Moho reflections, while the latter will induce gradual changes in acoustic impedance resulting in weak or no Moho reflections. We suggest that thick crust and thick dunite layers could be simultaneously generated by hydrous melting of the upper mantle. We discuss the crust formation process at MORs, and propose that faults, developing as the crust forms, can enable seawater, that otherwise rarely penetrates that far, to reach the mantle. This promotes mantle melting and results in thicker crust and thick dunite layers. This new hypothesis explains the origin of the Moho based on seismological and petrological observations, and could be considered as a revised 3D Penrose model.

Direct drilling and sampling of the Moho is the best way to test this hypothesis. However, it will require different types of oceanic crust to be sampled to compare MORBs and understand the petrologic origins of the crust–mantle boundary in different MOR settings.

ACKNOWLEDGMENTS

This work was supported by JSPS KAKENHI Grant Numbers JP17H02987, JP16H06347, JP16H02742, and JP21H01195. We are grateful to Profs. Peter Kelemen, Adam Kent, and Tom Sisson for critical reading of the early version of the manuscript. We thank Dr. Akira Ishiwatari and two anonymous reviewers for their careful and insightful reviews. Dr. Naoto Hirano is thanked for his editorial help. Seafloor bathymetric data in Figure 2 are ETOPO1 (Amante & Eakins, 2009). These figures were plotted using the Genie Mapping Tool. All the seismic survey data and multi narrow beam echo sounder data of JAMSTEC can be requested from JAMSTEC crustal structural database site (https://www.jamstec.go.jp/obsmcs_db/e/).

CONFLICT OF INTEREST

The authors declare no conflict of interest.

ORCID

Yoshihiko Tamura  <https://orcid.org/0000-0002-3705-7815>

Mathieu Rospabé  <https://orcid.org/0000-0002-6089-3475>

Gou Fujie  <https://orcid.org/0000-0002-6292-7034>

Akane Ohira  <https://orcid.org/0000-0002-7470-1825>

Kentaro Kaneda  <https://orcid.org/0000-0001-8890-9304>

Alexander R. L. Nichols  <https://orcid.org/0000-0002-8298-2882>

Georges Ceuleneer  <https://orcid.org/0000-0002-6198-4205>

Tomoki Sato  <https://orcid.org/0000-0002-0076-0531>

Shuichi Kodaira  <https://orcid.org/0000-0002-5774-2561>

Seiichi Miura  <https://orcid.org/0000-0002-9009-6039>

Eiichi Takazawa  <https://orcid.org/0000-0003-4004-6698>

REFERENCES

- Abily, B., & Ceuleneer, G. (2013). The dunitic mantle-crust transition zone in the Oman ophiolite: Residue of melt-rock interaction, cumulates from high-MgO melts, or both? *Geology*, *41*, 67–70.
- Abily, B., Ceuleneer, G., & Launeau, P. (2011). Synmagmatic normal faulting in the lower oceanic crust: Evidence from the Oman ophiolite. *Geology*, *39*, 391–394.
- Aghaei, O., Nedimović, M. R., Carton, H., Carbotte, S. M., Canales, J. P., & Mutter, J. C. (2014). Crustal thickness and Moho character of the fast-spreading East Pacific rise from 9°42'N to 9°57'N from poststack-migrated 3-D MCS data. *Geochemistry, Geophysics, Geosystems*, *15*, 634–657. <https://doi.org/10.1002/2013GC005069>
- Akizawa, N., Ozawa, K., Tamura, A., Michibayashi, K., & Arai, S. (2016). Three-dimensional evolution of melting, heat and melt transfer in ascending mantle beneath a fast spreading ridge segment constrained by trace elements in clinopyroxene from concordant dunites and host harzburgites of the Oman ophiolite. *Journal of Petrology*, *57*, 777–814. <https://doi.org/10.1093/petrology/egw020>
- Alt, J. C., Honnorez, J., Laverne, C., & Emmermann, R. (1986). Hydrothermal alteration of a 1-km section through the upper oceanic-crust, Deep Sea Drilling Project Hole 504B: Mineralogy, chemistry and evolution of seawater-basalt interactions. *Journal of Geophysical Research*, *91*, 10309–10335.
- Amante, C., & Eakins, B. W. (2009). *ETOPO1 1 arc-minute global relief model: Procedures, data sources and analysis*. NOAA technical memorandum NESDIS NGDC-24. National Geophysical Data Center, NOAA. <https://doi.org/10.7289/V5C8276M>
- Amri, I., Benoit, M., & Ceuleneer, G. (1996). Tectonic setting for the genesis of oceanic plagiogranites: Evidence from a paleo-spreading structure in the Oman ophiolite. *Earth and Planetary Science Letters*, *139*, 177–194.
- Arai, S. (2010). Possible recycled origin for ultrahigh-pressure chromitites in ophiolites. *Journal of Mineralogical and Petrological Sciences*, *105*, 280–285.
- Arai, S. (2013). Conversion of low-pressure chromitites to ultrahigh-pressure chromitites by deep recycling: A good inference. *Earth and Planetary Science Letters*, *379*, 81–87.
- Benn, K., Nicolas, A., & Reuber, I. (1988). Mantle-crust transition zone and origin of wehrlitic magmas: Evidence from the Oman ophiolite. *Tectonophysics*, *151*, 75–85.
- Benoit, M., Ceuleneer, G., & Polvé, M. (1999). The remelting of hydrothermally altered peridotite at mid-ocean ridges by intruding mantle diapirs. *Nature*, *402*, 514–518.
- Benoit, M., Polvé, M., & Ceuleneer, G. (1996). Trace element and isotopic characterization of mafic cumulates in a fossil mantle diapir (Oman ophiolite). *Chemical Geology*, *134*, 199–214.
- Bonatti, E., & Honnorez, J. (1976). Sections of the Earth's crust in the equatorial Atlantic. *Journal of Geophysical Research*, *81*, 4104–4116.
- Bonatti, E., Ligi, M., Brunelli, D., Cipriani, A., Fabretti, P., Ferrante, V., Gasperini, L., & Ottolini, L. (2003). Mantle thermal pulses below the mid-Atlantic ridge and temporal variations in the formation of oceanic lithosphere. *Nature*, *423*, 499–505.
- Borisova, A. Y., Ceuleneer, G., Kamenetsky, V. S., Arai, S., Bějina, F., Abily, B., Bindeman, I. N., Polvé, M., & Pokrovski, G. S. (2012). A new view on the petrogenesis of the Oman ophiolite chromitites from microanalyses of chromite-hosted inclusions. *Journal of Petrology*, *53*, 2411–2440.
- Boudier, F., & Nicolas, A. (1985). Harzburgite and lherzolite subtypes in ophiolitic and oceanic environments. *Earth and Planetary Science Letters*, *76*, 84–92.
- Boudier, F., & Nicolas, A. (1995). Nature of the Moho transition zone in the Oman ophiolite. *Journal of Petrology*, *36*, 777–796.
- Boudier, F., Nicolas, A., Ildefonse, B., & Jousset, D. (1997). EPR micro-plates, a model for the Oman ophiolite. *Terra Nova*, *9*, 79–82.
- Brocher, T. M., Karson, J. A., & Collins, J. A. (1985). Seismic stratigraphy of the oceanic Moho based on ophiolite models. *Geology*, *13*, 62–65.
- Cannat, M. (1993). Emplacement of mantle rocks in the seafloor at mid-ocean ridges. *Journal of Geophysical Research*, *98*, 4163–4172.
- Cannat, M. (1996). How thick is the magmatic crust at slow spreading oceanic ridges? *Journal of Geophysical Research: Solid Earth*, *101*, 2847–2857.
- Cannat, M., Bideau, D., & Hébert, R. (1990). Plastic deformation and magmatic impregnation in serpentinized ultramafic rocks from the Garrett transform fault (East Pacific Rise). *Earth and Planetary Science Letters*, *101*, 216–232.
- Cannat, M., Lagabriele, Y., Bougault, H., Casey, J., de Coutures, N., Dmitriev, L., & Fouquet, Y. (1997). Ultramafic and gabbroic exposures at the mid-Atlantic ridge: Geologic mapping in the 15° N region. *Tectonophysics*, *279*, 193–213.
- Ceuleneer, G. (1986). Structure des ophiolites d'Oman: flux mantellaire sous un centre d'expansion océanique et charriage à la dorsale. PhD thesis, Université de Nantes, 349 pp.
- Ceuleneer, G. (1991). Evidence for a paleo-spreading center in the Oman ophiolite: Mantle structures in the Maqсад area. In *Ophiolite genesis and evolution of the oceanic lithosphere* (pp. 147–173). Springer.
- Ceuleneer, G., Monnereau, M., & Amri, I. (1996). Thermal structure of a fossil mantle diapir inferred from the distribution of mafic cumulates. *Nature*, *379*, 149–153.
- Ceuleneer, G., & Nicolas, A. (1985). Structures in podiform chromite from the Maqсад district (Sumail ophiolite, Oman). *Mineralium Deposita*, *20*, 177–185.
- Ceuleneer, G., Nicolas, A., & Boudier, F. (1988). Mantle flow patterns at an oceanic spreading Centre: The Oman peridotites record. *Tectonophysics*, *151*, 1–26.
- Christensen, N. I., & Smewing, H. D. (1981). Geology and seismic structure of the northern section of the Oman ophiolite. *Journal of Geophysical Research*, *86*, 2545–2555.
- Cipriani, A., Bonatti, E., Brunelli, D., & Ligi, M. (2009). 26 million years of mantle upwelling below a segment of the mid Atlantic ridge: The Vema lithospheric section revisited. *Earth and Planetary Science Letters*, *285*, 87–95.
- Clénet, H., Ceuleneer, G., Pinet, P., Abily, B., Daydou, Y., Harris, E., Amri, I., & Dantas, C. (2010). Thick sections of layered ultramafic cumulates in the Oman ophiolite revealed by an airborne hyperspectral survey: Petrogenesis and relationship to mantle diapirism. *Lithos*, *114*, 265–281.
- Coleman, R. G. (1971). Petrologic and geophysical nature of serpentinites. *Geological Society of America Bulletin*, *82*, 897–918.
- Collins, J. A., Brocher, T. M., & Karson, J. A. (1986). Two-dimensional seismic reflection modeling of the inferred fossil oceanic crust/mantle transition in the bay of Island ophiolite. *Journal of Geophysical Research*, *91*, 12520–12538.
- Conference participants. (1972). Penrose field conference ophiolites. *Geotimes*, *17*, 24–25.
- Dewey, J. F., & Bird, J. M. (1971). Origin and emplacement of the ophiolite suite: Appalachian ophiolites in Newfoundland. *Journal of Geophysical Research*, *76*, 3179–3206.
- Dick, H. J. (1977). Evidence of partial melting in the Josephine peridotite. *State of Oregon Department of Geology and Mineral Industries Bulletin*, *96*, 384–422.
- Dick, H. J., Lin, J., & Schouten, H. (2003). An ultraslow-spreading class of ocean ridge. *Nature*, *426*, 405–412.
- Dick, H. J., Natland, J. H., & Ildefonse, B. (2006). Past and future impact of deep drilling in the oceanic crust and mantle. *Oceanography*, *19*, 72–80.

- Dilek, Y. (2003). Ophiolite concept and its evolution. *Geological Society of America Special Paper*, 373, 1–16.
- Dilek, Y., & Furnes, H. (2011). Ophiolite genesis and global tectonics: Geochemical and tectonic fingerprinting of ancient oceanic lithosphere. *Geological Society of America Bulletin*, 123, 387–411. <https://doi.org/10.1130/B30446.1>
- Dunn, R. A., Toomey, D. R., & Solomon, S. C. (2000). Three-dimensional seismic structure and physical properties of the crust and shallow mantle beneath the East Pacific rise at 9°30' N. *Journal of Geophysical Research*, 105, 23537–23555.
- France, L., Ildefonse, B., & Koepke, J. (2009). Interactions between magma and hydrothermal system in Oman ophiolite and in IODP hole 1256D: Fossilization of a dynamic melt lens at fast spreading ridges. *Geochemistry, Geophysics, Geosystems*, 10, Q10019. <https://doi.org/10.1029/2009GC002652>
- France, L., Ildefonse, B., & Koepke, J. (2013). Hydrous magmatism triggered by assimilation of hydrothermally altered rocks in fossil oceanic crust (northern Oman ophiolite). *Geochemistry, Geophysics, Geosystems*, 14, 2598–2614. <https://doi.org/10.1002/ggge.20137>
- Fujie, G., Kodaira, S., Kaiho, Y., Yamamoto, Y., Takahashi, T., Miura, S., & Yamada, T. (2018). Controlling factor of incoming plate hydration at the North-Western Pacific margin. *Nature Communications*, 9, 3844. <https://doi.org/10.1038/s41467-018-06320-z>
- Fujie, G., Kodaira, S., Nakamura, Y., Morgan, J. P., Dannowski, A., Thorwart, M., Grevemeyer, I., & Miura, S. (2020). Spatial variations of incoming sediments at the northeastern Japan arc and their implications for megathrust earthquakes. *Geology*, 48, 614–619.
- Fujie, G., Kodaira, S., Yamashita, M., Sato, T., Takahashi, T., & Takahashi, N. (2013). Systematic changes in the incoming plate structure at the Kuril trench. *Geophysical Research Letters*, 40, 88–93. <https://doi.org/10.1029/2012GL054340>
- Godard, M., Jousselin, D., & Bodinier, J. L. (2000). Relationships between geochemistry and structure beneath a palaeo-spreading Centre: A study of the mantle section in the Oman ophiolite. *Earth and Planetary Science Letters*, 180, 133–148.
- Grove, T. L., Kinzler, R. J., & Bryan, W. B. (1992). Fractionation of mid-ocean ridge basalt. In J. P. Morgan, D. K. Blackman, & J. M. Sinton (Eds.), *Mantle flow and melt generation at Mid-Ocean ridges* (Vol. 71, pp. 281–311). American Geophysical Union Monograph.
- Hess, H. H. (1962). History of ocean basins. In F. Buddington, A. E. J. Engel, H. L. James, & B. F. Leonard (Eds.), *Petrologic studies: A volume in honor of A* (pp. 599–620). Geological Society of America.
- Ildefonse, B., Blackman, D. K., John, B. E., Ohara, Y., Miller, D. J., & MacLeod, C. J. (2007). Oceanic core complexes and crustal accretion at slow-spreading ridges. *Geology*, 35, 623–626.
- Ishiwatari, A. (1985a). Alpine ophiolites: Product of low-degree mantle melting in a Mesozoic transcurrent rift zone. *Earth and Planetary Science Letters*, 76, 93–108.
- Ishiwatari, A. (1985b). Igneous petrogenesis of the Yakuno ophiolite (Japan) in the context of the diversity of ophiolites. *Contributions to Mineralogy and Petrology*, 89, 155–167.
- Ishiwatari, A. (2010). New developments in ophiolites studies. *Journal of Geography*, 119, 841–851 (in Japanese with English abstract).
- Jarchow, C. M., & Thompson, G. A. (1989). The nature of the Mohorovičić discontinuity. *Annual Reviews of Earth and Planetary Sciences*, 17, 475–506.
- Jousselin, D., & Nicolas, A. (2000). The Moho transition zone in the Oman ophiolite-relation with wehrlites in the crust and dunites in the mantle. *Marine Geophysical Researches*, 21, 229–241.
- Juteau, T., Ernwein, M., Reuber, I., Whitechurch, H., & Dahl, R. (1988). Duality of magmatism in the plutonic sequence of the Sumail Nappe, Oman. *Tectonophysics*, 151, 107–135.
- Kaneda, K., Kodaira, S., Nishizawa, A., Morishita, T., & Takahashi, N. (2010). Structural evolution of preexisting oceanic crust through intra-plate igneous activities in the Marcus-Wake seamount chain. *Geochemistry, Geophysics, Geosystems*, 11, 1–29. <https://doi.org/10.1029/2010GC003231>
- Katayama, I., Abe, N., Hatakeyama, K., Akamatsu, Y., Okazaki, K., Ulven, O. I., Hong, G., Zhu, W., Cordonnier, B., Michibayashi, K., & Godard, M. (2020). Permeability profiles across the crust-mantle sections in the Oman drilling project inferred from dry and wet resistivity data. *Journal of Geophysical Research: Solid Earth*, 125, e2019JB018698.
- Kelemen, P. B. (1990). Reaction between ultramafic rock and fractionating basaltic magma I. phase relations, the origin of calc-alkaline magma series, and the formation of discordant dunite. *Journal of Petrology*, 31, 51–98.
- Kelemen, P. B., Matter, J. M., Teagle, D. A. H., Coggon, J. A., & the Oman Drilling Project Science Team. (2020). Proceedings of the Oman drilling project: College Station, TX (International Ocean Discovery Program). <https://doi.org/10.14379/OmanDP.proc.2020>.
- Kelemen, P. B., Shimizu, N., & Salters, V. J. M. (1995). Extraction of mid-ocean-ridge basalt from the upwelling mantle by focused flow of melt in dunite channels. *Nature*, 375, 747–753.
- Kempner, W., & Gettrust, J. F. (1982). Ophiolites, synthetic seismograms, and oceanic crustal structure 2. A comparison of synthetic seismograms of the Samail ophiolite, Oman, and the ROSE refraction data from the East Pacific rise. *Journal of Geophysical Research*, 87, 8463–8476.
- Kodaira, S., Fujie, G., Yamashita, M., Sato, T., Takahashi, T., & Takahashi, N. (2014). Seismological evidence of mantle flow driving plate motions at a palaeo-spreading Centre. *Nature Geoscience*, 7, 371–375. <https://doi.org/10.1038/ngeo2121>
- Koepke, J., Berndt, J., Feig, S. T., & Holtz, F. (2007). The formation of SiO₂-rich melts within the deep oceanic crust by hydrous partial melting of gabbros. *Contributions to Mineralogy and Petrology*, 153, 67–84.
- Koepke, J., Berndt, J., Horn, I., Fahle, J., & Wolff, P. E. (2014). Partial melting of oceanic gabbro triggered by migrating water-rich fluids: A prime example from the Oman ophiolite. *Geological Society, London, Special Publications*, 392, 195–212.
- Koepke, J., Feig, S. T., & Snow, J. (2005). Hydrous partial melting within the lower oceanic crust. *Terra Nova*, 17, 286–291.
- Koepke, J., Schoenborn, S., Oelze, M., Wittmann, H., Feig, S. T., Hellebrand, E., Boudier, F., & Schoenberg, R. (2009). Petrogenesis of crustal wehrlites in the Oman ophiolite: Experiments and natural rocks. *Geochemistry Geophysics Geosystems*, 10, Q10002. <https://doi.org/10.1029/2009GC002488>
- Koga, K. T., Kelemen, P. B., & Shimizu, N. (2001). Petrogenesis of the crust-mantle transition zone and the origin of lower crustal wehrlite in the Oman ophiolite. *Geochemistry, Geophysics, Geosystems*, 2, 2000GC000132.
- Lee, W. H. K., & Uyeda, S. (1965). Chapter 6. Review of heat flow data. *Geophysical Monograph Series*, 8, 87–190.
- Lian, D., & Yang, J. (2019). Ophiolite-hosted diamond: A new window for probing carbon cycling in the deep mantle. *Engineering*, 5, 406–420. <https://doi.org/10.1016/j.eng.2019.02.006>
- MacLeod, C. J., & Rothery, D. A. (1992). Ridge axial segmentation in the Oman ophiolite: Evidence from along-strike variations in the sheeted dyke complex. *Geological Society, London, Special Publications*, 60, 39–63.
- Maia, M., Sichel, S., Briaes, A., Brunelli, D., Ligi, M., Ferreira, N., Campos, T., Mougél, B., Brehme, I., Hémond, C., & Motoki, A. (2016). Extreme mantle uplift and exhumation along a transpressive transform fault. *Nature Geoscience*, 9, 619–623.
- Mével, C., Cannat, M., Gente, P., Marion, E., Auzende, J. M., & Karson, J. A. (1991). Emplacement of deep crustal and mantle rocks on the west median valley wall of the MARK area (MAR, 23 N). *Tectonophysics*, 190, 31–53.
- Michibayashi, K., Tominaga, M., Ildefonse, B., & Teagle, D. A. (2019). What lies beneath the formation and evolution of oceanic lithosphere. *Oceanography*, 32, 138–149.

- Minshull, T. A., Muller, M. R., Robinson, C. J., White, R. S., & Bickle, M. J. (1998). Is the oceanic Moho a serpentinization front? *Geological Society, London, Special Publications*, 148, 71–80.
- Miura, M., Arai, S., Ahmed, A. H., Mizukami, T., Okuno, M., & Yamamoto, S. (2012). Podiform chromitite classification revisited: A comparison of discordant and concordant chromitite pods from Wadi Hilti, northern Oman ophiolite. *Journal of Asian Earth Sciences*, 59, 52–61.
- Miyashiro, A. (1973). The Troodos ophiolitic complex was probably formed in an Island arc. *Earth and Planetary Science Letters*, 25, 217–222.
- Mohorovičić, A. (1910). Potres od 8/X 1909. (Das Beben vom 8.X. 1909). *Jahrbuch des meteorologischen Observatoriums in Zagreb (Agram) für das Jahr, 1909*, 1–56.
- Mutter, J. C., & Carton, H. D. (2013). The Mohorovičić discontinuity in ocean basins: Some observations from seismic data. *Tectonophysics*, 609, 314–330.
- Nakanishi, M. (2017). Bending-related topographic structures of the incoming oceanic plate at the northwestern Pacific Ocean trench. *Journal of Geography (Chigaku Zasshi)*, 126, 125–146.
- Nakanishi, M., Tamaki, K., & Kobayashi, K. (1992). Magnetic anomaly lineations from late Jurassic to early cretaceous in the west-Central Pacific Ocean. *Geophysical Journal International*, 109, 701–719.
- Nicolas, A., Boudier, F., & France, L. (2009). Subsidence in magma chamber and the development of magmatic foliation in Oman ophiolite gabbros. *Earth and Planetary Science Letters*, 284, 76–87.
- Nicolas, A., Boudier, F., & Ildefonse, B. (1996). Variable crustal thickness in the Oman ophiolite: Implication for oceanic crust. *Journal of Geophysical Research*, 101, 17941–17950.
- Nicolas, A., Ceuleneer, G., Boudier, F., & Misseri, M. (1988). Structural mapping in the Oman ophiolites: Mantle diapirism along an oceanic ridge. *Tectonophysics*, 151, 27–56.
- Nonnotte, P., Ceuleneer, G., & Benoit, M. (2005). Genesis of andesitic–boninitic magmas at mid-ocean ridges by melting of hydrated peridotites: Geochemical evidence from DSDP site 334 gabbro-norites. *Earth and Planetary Science Letters*, 236, 632–653.
- Ohira, A., Kodaira, S., Nakamura, Y., Fujie, G., Arai, R., & Miura, S. (2017). Structural variation of the oceanic Moho in the Pacific plate revealed by active-source seismic data. *Earth and Planetary Science Letters*, 476, 111–121.
- Oliver, J. (1982). Changes at the crust–mantle boundary. *Nature*, 299, 398–399.
- O'Reilly, B. M., Hauser, F., Jacob, A. W. B., & Shannon, P. M. (1996). The lithosphere below the Rockall trough: Wide-angle seismic evidence for extensive serpentinisation. *Tectonophysics*, 255, 1–23.
- O'Reilly, S. Y., & Griffin, W. L. (2013). Moho vs crust–mantle boundary: Evolution of an idea. *Tectonophysics*, 609, 535–546.
- Pallister, J. S., & Hopson, C. A. (1981). Samail ophiolite plutonic suite: Field relations, phase variation, cryptic variation and layering, and a model of a spreading ridge magma chamber. *Journal of Geophysical Research: Solid Earth*, 86, 2593–2644.
- Pearce, J. A., & Robinson, P. T. (2010). The Troodos ophiolitic complex probably formed in a subduction initiation, slab edge setting. *Gondwana Research*, 18, 60–81. <https://doi.org/10.1016/j.gr.2009.12.003>
- Presnall, D. C., Dixon, J. R., O'Donnel, T. H., & Dixon, S. A. (1979). Generation of mid-ocean ridge tholeiites. *Journal of Petrology*, 20, 3–35.
- Prodehl, C., Kennett, B., Artemieva, I. M., & Thybo, H. (2013). 100 years of seismic research on the Moho. *Tectonophysics*, 609, 9–44.
- Python, M., & Ceuleneer, G. (2003). Nature and distribution of dykes and related melt migration structures in the mantle section of the Oman ophiolite. *Geochemistry, Geophysics, Geosystems*, 4, 8612. <https://doi.org/10.1029/2002GC000354>
- Python, M., Ceuleneer, G., & Arai, S. (2008). Chromian spinels in mafic–ultramafic mantle dykes: Evidence for a two-stage melt production during the evolution of the Oman ophiolite. *Lithos*, 106, 137–154.
- Rabinowicz, M., & Ceuleneer, G. (2005). The effect of sloped isotherms on melt migration in the shallow mantle: A physical and numerical model based on observations in the Oman ophiolite. *Earth and Planetary Science Letters*, 229, 231–246.
- Rabinowicz, M., Ceuleneer, G., & Nicolas, A. (1987). Melt segregation and flow in mantle diapirs below spreading centers: Evidence from the Oman ophiolite. *Journal of Geophysical Research*, 92, 3475–3486.
- Rioux, M., Bowring, S., Kelemen, P., Gordon, S., Dudás, F., & Miller, R. (2012). Rapid crustal accretion and magma assimilation in the Oman–UAE ophiolite: High precision U–Pb zircon geochronology of the gabbroic crust. *Journal of Geophysical Research: Solid Earth*, 117, B07201. <https://doi.org/10.1029/2012JB009273>
- Rioux, M., Bowring, S., Kelemen, P., Gordon, S., Miller, R., & Dudás, F. (2013). Tectonic development of the Samail ophiolite: High-precision U–Pb zircon geochronology and Sm–Nd isotopic constraints on crustal growth and emplacement. *Journal of Geophysical Research: Solid Earth*, 118, 2085–2101.
- Rioux, M., Garber, J., Bauer, A., Bowring, S., Searle, M., Kelemen, P., & Hacker, B. (2016). Synchronous formation of the metamorphic sole and igneous crust of the Semail ophiolite: New constraints on the tectonic evolution during ophiolite formation from high-precision U–Pb zircon geochronology. *Earth and Planetary Science Letters*, 451, 185–195.
- Robinson, P. T., Bai, W.-J., Malpas, J., Yang, J.-S., Zhou, M. F., Fang, Q.-S., Hu, X.-F., Cameron, S., & Staudigel, H. (2004). Ultra-high pressure minerals in the Luobusa ophiolite, Tibet, and their tectonic implications. In J. Malpas, C. J. N. Fletcher, J. R. Ali, & H. C. Aitchison (Eds.), *Aspects of the tectonic evolution of China* (Vol. 226, pp. 247–271). Geological Society.
- Rospabé, M. (2018). Etude pétrologique, géochimique et structurale de la zone de transition dunitique dans l'ophiolite d'Oman: Identification des processus pétrogénétiques à l'interface manteau/croûte. PhD thesis, Université Paul Sabatier, Toulouse III, 628 pp.
- Rospabé, M., Benoit, M., Ceuleneer, G., Hodel, F., & Kaczmarek, M. A. (2018). Extreme geochemical variability through the dunitic transition zone of the Oman ophiolite: Implications for melt/fluid–rock reactions at Moho level beneath oceanic spreading centers. *Geochimica et Cosmochimica Acta*, 234, 1–23.
- Rospabé, M., Benoit, M., Ceuleneer, G., Kaczmarek, M. A., & Hodel, F. (2019). Melt hybridization and metasomatism triggered by syn-magmatic faults within the Oman ophiolite: A clue to understand the genesis of the dunitic mantle–crust transition zone. *Earth and Planetary Science Letters*, 516, 108–121.
- Rospabé, M., Ceuleneer, G., Benoit, M., Abily, B., & Pinet, P. (2017). Origin of the dunitic mantle–crust transition zone in the Oman ophiolite: The interplay between percolating magmas and high-temperature hydrous fluids. *Geology*, 45, 471–474.
- Rospabé, M., Ceuleneer, G., Benoit, M., & Kaczmarek, M. A. (2020). Composition gradients in silicate inclusions in chromites from the dunitic mantle–crust transition (Oman ophiolite) reveal high temperature fluid–melt–rock interaction controlled by faulting. *Ophioliti*, 45, 103–114.
- Rospabé, M., Ceuleneer, G., Granier, N., Arai, S., & Borisova, A. Y. (2019). Multi-scale development of a stratiform chromite ore body at the base of the dunitic mantle–crust transition zone (Maqсад diapir, Oman ophiolite): The role of repeated melt and fluid influxes. *Lithos*, 350, 105235.
- Sauter, D., Cannat, M., Rouméjon, S., Andreani, M., Birot, D., Bronner, A., Brunelli, D., Carlut, J., Delacour, A., Guyader, V., & MacLeod, C. J. (2013). Continuous exhumation of mantle-derived rocks at the southwest Indian ridge for 11 million years. *Nature Geoscience*, 6, 314–320.
- Singh, S. C., Harding, A. J., Kent, G. M., Sinha, M. C., Combier, V., Bazin, S., Tong, C. H., Pye, J. W., Barton, P. J., Hobbs, R. W., White, R. S., & Orcutt, J. A. (2006). Seismic reflection images of the Moho underlying melt sills at the East Pacific rise. *Nature*, 442, 287–290. <https://doi.org/10.1038/nature04939>
- Smewing, J. D. (1981). Mixing characteristics and compositional differences in mantle-derived melts beneath spreading axes: Evidence from

- cyclically layered rocks in the ophiolite of North Oman. *Journal of Geophysical Research: Solid Earth*, 86, 2645–2659.
- Stoffa, P. L., Buhl, P., Herron, T. J., Kan, T. K., & Ludwig, W. J. (1980). Mantle reflections beneath the crestral zone of the East Pacific rise from multi-channel seismic data. *Marine Geology*, 35, 83–97.
- Stolper, E. (1980). A phase diagram for Mid-Ocean ridge basalts: Preliminary results and implications for petrogenesis. *Contributions to Mineralogy and Petrology*, 74, 13–27.
- Tamura, Y., Ishizuka, O., Sato, T., & Nichols, A. R. L. (2019). Nishinoshima volcano in the Ogasawara arc: New continent from the ocean? *Island Arc*, 28, e12285. <https://doi.org/10.1111/iar.12285>
- Tamura, Y., Sato, T., Fujiwara, T., Kodaira, S., & Nichols, A. (2016). Advent of continents: A new hypothesis. *Scientific Reports*, 6, 33517. <https://doi.org/10.1038/srep33517>
- Tilton, G. R., Hopson, C. A., & Wright, J. E. (1981). Uranium-lead isotopic ages of the Samail ophiolite, Oman, with applications to Tethyan Ocean ridge tectonics. *Journal of Geophysical Research: Solid Earth*, 86, 2763–2775.
- Tippit, P. R., Pessagno, E. A., & Smewing, J. D. (1981). The biostratigraphy of sediments in the volcanic unit of the Samail ophiolite. *Journal of Geophysical Research: Solid Earth*, 86, 2756–2762.
- Wanless, V. D., Perfit, M. R., Ridley, W. I., & Klein, E. (2010). Dacite petrogenesis on mid-ocean ridges: Evidence for oceanic crustal melting and assimilation. *Journal of Petrology*, 51, 2377–2410.
- Wolff, P. E., Koepke, J., & Feig, S. T. (2013). The reaction mechanism of fluid-induced partial melting of gabbro in the oceanic crust. *European Journal of Mineralogy*, 25, 279–298.
- Yamamoto, S., Komiya, T., Hirose, K., & Maruyama, S. (2009). Coesite and clinopyroxene exsolution lamellae in chromites: In-situ ultrahigh-pressure evidence from Podiform chromites in the Luobusa ophiolite, southern Tibet. *Lithos*, 109, 314–322.
- Yamane, N., Kanagawa, K., & Ito, T. (2012). Contrasting seismic reflectivity of the lower crust and uppermost mantle between NE Japan and SW Japan as illustrated by petrophysical analyses of mafic and ultramafic xenoliths. *Journal of Geophysical Research*, 117, B09203. <https://doi.org/10.1029/2011JB009008>
- Yang, J.-S., Dobrzhinetskaya, L., Bai, W.-J., Fang, Q.-S., Robinson, P. T., Zhang, J., & Green, H. W., II. (2007). Diamond- and coesite-bearing chromitites from the Luobusa ophiolite, Tibet. *Geology*, 35, 875–878.
- Yao, Y., Takazawa, E., Chatterjee, S., Richard, A., Merlot, C., Créon, L., Al-Busaidi, S., Michibayashi, K., & Oman Drilling Project Science Team. (2020). High resolution X-ray computed tomography and scanning electron microscopy studies of multiphase solid inclusions in Oman podiform chromitite: Implications for post-entrapment modification. *Journal of Mineralogical and Petrological Sciences*, 115, 247–260.
- Zhang, C., Koepke, J., France, L., & Godard, M. (2017). Felsic plutonic rocks from IODP hole 1256D, eastern Pacific: Implications for the nature of the axial melt lens at fast-spreading mid-ocean ridges. *Journal of Petrology*, 58, 1535–1565.
- Zihlmann, B., Müller, S., Coggon, R. M., Koepke, J., Garbe-Schönberg, D., & Teagle, D. A. (2018). Hydrothermal fault zones in the lower oceanic crust: An example from Wadi Gideah, Samail ophiolite, Oman. *Lithos*, 323, 103–124.

How to cite this article: Tamura, Y., Rospabé, M., Fujie, G., Ohira, A., Kaneda, K., Nichols, A. R. L., Ceuleneer, G., Sato, T., Kodaira, S., Miura, S., & Takazawa, E. (2022). The nature of the Moho beneath fast-spreading centers: Evidence from the Pacific plate and Oman ophiolite. *Island Arc*, 31(1), e12460. <https://doi.org/10.1111/iar.12460>